FALL 2024
electronics-cooling.com

electronics COOLING

FEATURED IN THIS EDITION

12 THE CRITICAL RADIUS IN CYLINDRICAL SYSTEMS

14 A NON-CONTACT MEASUREMENT METHOD FOR THIN VAPOR CHAMBERS BY PHOTONICS TECHNOLOGIES

18 POWER DENSITY IN THE CONTEXT OF TWO-PHASE IMMERSION COOLING

24 THETA-JC MEASUREMENTS: STEADY-STATE COMPARED TO TRANSIENT METHODS

6 SUMMARY OF SEMI-THERM 40 CONFERENCE

9 TECH BRIEF
THERMOCOUPLE TRANSIENT BEHAVIOR

CONTENTS

electronics COOLING
electronics-cooling.com

3 **EDITORIAL**
Alex Ockfen

4 **TECHNICAL EDITORS SPOTLIGHT**

5 **COOLING EVENTS**
News of Upcoming 2024 Thermal Management Events

6 **SUMMARY OF SEMI-THERM 40 CONFERENCE**
Navid Kazem, Lieven Vervecken, and Alex Ockfen, P.E.

9 **TECH BRIEF**
Thermocouple Transient Behavior
Ross Wilcoxon

12 **THE CRITICAL RADIUS IN CYLINDRICAL SYSTEMS**
James Petroski

14 **A NON-CONTACT MEASUREMENT METHOD FOR THIN VAPOR CHAMBERS BY PHOTONICS TECHNOLOGIES**
Kuang-Yu Hsu, PhD

18 **POWER DENSITY IN THE CONTEXT OF TWO-PHASE IMMERSION COOLING**
Jimil M. Shah, PhD and Phillip E. Tuma

24 **THETA jc MEASUREMENTS: STEADY-STATE COMPARED TO TRANSIENT METHODS**
Jesse Galloway and Robin Bornoff

31 **INDEX OF ADVERTISERS**

PUBLISHED BY
Lectrix
716 Dekalb Pike, #351
Blue Bell, PA 19422
Phone: +1 484-688-0300
info@lectrixgroup.com
lectrixgroup.com

CHIEF EXECUTIVE OFFICER
Graham Kilshaw | graham@lectrixgroup.com

DIRECTOR OF BUSINESS DEVELOPMENT
Ashlee Zapata-McCants | ashlee@lectrixgroup.com

CREATIVE DIRECTOR
Kate Teti | kate@lectrixgroup.com

GRAPHIC DESIGNER
Marcos Cruz | marcos@lectrixgroup.com

DELIVERY MANAGER
Mackenzie Mann | mackenzie@lectrixgroup.com

▶**SUBSCRIPTIONS ONLINE**
at electronics-cooling.com

For subscription changes email
info@electronics-cooling.com

FREE SUBSCRIPTIONS

Lectrix®, Electronics Cooling®—The **2024 Fall Edition** is distributed digitally at no charge to engineers and managers engaged in the application, selection, design, test, specification or procurement of electronic components, systems, materials, equipment, facilities or related fabrication services. Subscriptions are available through electronics-cooling.com.

LECTRIX®

EDITORIAL

Alex Ockfen, P.E.
Associate Technical Editor of *Electronics Cooling Magazine*
Product Design Engineer, Meta

Welcome to the Fall issue of *Electronics Cooling Magazine*.

Curiosity is often defined as the desire to learn something new. This trait is common in children, with many children having an insatiable appetite for questions. Although the constant stream of questions can sometimes be overwhelming, I appreciate the curiosity and eagerness behind them. As we all advance through our education and professional careers, we learn best practices, iterate from existing solutions, and often are forced to put our heads down and focus on the task at hand. While these traits and processes are essential for a profession, such as engineering, that directly impacts people's livelihood and quality of life, they should not replace our curiosity. I always find myself energized or reinvigorated when I think outside the box. Often, these general curiosities have led me to professional insights that I would not have reached via traditional means.

A recent experience sparked this topic in my mind. During my run on a beautiful summer morning, I noticed a hot air balloon. What would it be like to be in that balloon up there? The cool air at altitude being a welcome relief to my run. Over a few miles, the wind pushed the balloon along my path, allowing me to watch it slowly descend.

Being surrounded by a river, fields, and wooded areas; I began to get nervous as the balloon drifted towards various obstacles during its descent. As the balloon approached, I began to see the balloon's pilot periodically operate the burner to change the air temperature in the balloon, increasing or decreasing its buoyant force. The pilot's maneuvers led me to consider the thermal time constant at play as the air in the balloon heated and cooled to control its altitude.

Yes, I am already familiar with the working principles at play. Yet, being there in person—observing the nuances of hot air balloon navigation—sparked my interest. I began brainstorming about how buoyancy, Charles law, the variation of air pressure with altitude, center of gravity, center of buoyancy, and other principles could be leveraged to solve other problems in my day-to-day life. While I can't say this led to an immediate breakthrough, it sparked my interest and curiosity, energizing me through the rest of my day. Perhaps observing biomimicry during a hike will lead you to a breakthrough or a rapidly evolving AI tool will inspire you. Whatever your interests, get out there, be curious, and find innovative solutions to new and existing thermal challenges.

This edition of *Electronics Cooling Magazine* includes a range of interesting articles that cover a diverse set of topics meant spark your curiosity, including: high power-density immersion cooling in data centers, a comparison of steady and transient package thermal resistance characterization methods, and a deep dive into non-contact measurement methods for vapor chambers. You will also find columns that help you tune up your fundamentals. Check them out to learn about the critical radius for cylindrical heat transfer problems, and thermocouple usage best practices for transient measurements.

I hope you enjoy the content in this issue. Don't hesitate to share feedback so we can continue improving. Thanks.

TECHNICAL EDITORS SPOTLIGHT

Meet the 2024 Editorial Board

VICTOR CHIRIAC, PhD | GLOBAL COOLING TECHNOLOGY GROUP

Associate Technical Editor

A fellow of the American Society of Mechanical Engineers (ASME) since 2014, Dr. Victor Adrian Chiriac is a co-founder and a managing partner with the Global Cooling Technology Group since 2019. He previously held technology/engineering leadership roles with Motorola (1999 – 2010), Qualcomm (2010 – 2018) and Huawei R&D USA (2018 – 2019). Dr. Chiriac was elected Chair of the ASME K-16 Electronics Cooling Committee and was elected the Arizona and New Mexico IMAPS Chapter President. He is a leading member of the organizing committees of ASME/InterPack, ASME/ IMECE and IEEE/CPMT Itherm Conferences. He holds 21 U.S. issued patents, 2 US Trade Secrets and 1 Defensive Publication (with Motorola), and has published over 110 papers in scientific journals and at conferences.

► vchiriac@gctg-llc.com

GENEVIEVE MARTIN | ASML

Associate Technical Editor

Genevieve Martin is a Senior Group Manager with ASML in the Netherlands. She has worked in the field of cooling of electronics and thermal management for over twenty years in different application fields. From 2016 to 2019, she coordinated the European project Delphi4LED, which dealt with multi-domain compact modeling of LEDs and, since 2021, is coordinating the AI-TWILIGHT project. She served as general chair of the SEMI-THERM conference and is an active reviewer and technical committee member in key conferences including SEMI-THERM, Therminic, and Eurosime. She has over 20 journal and conference papers and 16 worldwide patents.

► gmartin.sig1@gmail.com

ALEX OCKFEN, P.E. | META

Associate Technical Editor

Alex Ockfen is a product design engineer at Meta (formerly Facebook), providing technical leadership for thermal and structural design of consumer electronics products. He held previous positions at Raytheon where he obtained experience in thermal management and electronics cooling of a wide range of aerospace and defense applications. He has more than 10 journal and conference publications, is an inventor on multiple patents, is a professional mechanical engineer, and served as the program chair for SEMI-THERM in 2024.

► alex.ockfen@meta.com

ROSS WILCOXON | COLLINS AEROSPACE

Associate Technical Editor

Dr. Ross Wilcoxon is a Senior Technical Fellow in the Collins Aerospace Advanced Technology group. He conducts research and supports product development in the areas of component reliability, electronics packaging, and thermal management for communication, processing, displays, and radars. He has more than 40 journal and conference publications and is an inventor on more than 30 US Patents. Prior to joining Rockwell Collins (now Collins Aerospace) in 1998, he was an assistant professor at South Dakota State University.

► ross.wilcoxon@collins.com

COOLING EVENTS

News of Upcoming 2024 Thermal Management Events

SEP
25-27

THERMINIC 2024

Suburban Collection Showplace | Toulouse, France

THERMINIC is the major European Workshop related to thermal and reliability issues in electronic components and systems. For aca- demics and industrialists involved in micro and power electronics this annual event promises to be a very special occasion with a high quality technical programme and exciting social events.

► **therminic2024.eu**

SEP
25-27

MicDAT 2024

Ibiza Twiins Hotel | Ibiza, Spain

The conference is the 6th of Series of annual International Conferences on Microelectronic Devices and Technologies (MicDAT) held in Ibiza, Spain organized by IFSA - non-profit, professional association, serving for academy and industry since 1999. The MicDAT 2024 conference is intended to create awareness of the huge potential of modern microelectronic technologies and to improve understanding on the recent challenges in a wide range of applications. The many different technological bases for the fabrication of microelectronic devices, SoC, SiP, MEMS and NEMS will be outlined in this event. A number of recognized experts from both: academy and industry in the field of microelectronic design will be invited to give their view in selected application areas. Featuring strong participation of industry and academia, the MicDAT 2024 conference will provide an excellent opportunity to exchange ideas and present latest advancements in these areas.

► **micdat-conference.com**

OCT
7-10

THE BATTERY SHOW 2024

Huntington Place | Detroit, MI

The Battery Show and EVT Expo is moving! Now entering its 14th year, North America's largest advanced battery event will take over Huntington Place in Downtown Detroit this October. The Battery Show brings together engineers, business leaders, top-industry companies, and innovative thinkers to discover ground-breaking products and create powerful solutions for the future. More than 19,000 attendees are expected to take advantage of four full days of educational sessions, networking opportunities and, of course, explore the latest market innovations from over 1,150 exhibitors across one of the world's largest battery technology trade shows. Become part of this great event!

►**thebatteryshow.com**

Summary of SEMI-THERM 40 Conference

Navid Kazem
CEO and co-founder of Arieca Inc

Lieven Vervecken
CEO and Co-Founder of Diabatix

Alex Ockfen, P.E.
Product Design Engineer at Meta

The SEMI-THERM 40 Symposium was held March 25-28, 2024 at the Double Tree Hotel in San Jose, CA. Program organization was led by General Chair Alex Ockfen (Meta), Program Chair Dr. Lieven Vervecken (Diabatix), and Program Vice Chair Dr. Navid Kazem (Arieca). It featured a variety of activities including technical short courses, technical sessions, invited presentations, vendor exhibits and workshops, two panel discussions and two luncheon talks.

Short courses

Seven short courses were held on Monday, March 25. These courses were selected to provide learning opportunities for individuals ranging from those who are new to thermal design to those who are highly experienced. These courses were included:

- *"Semiconductor Packing and Thermals: Upcoming Challenges"*, taught by Dr. Kyle Arrington of Intel.
- *"Navigating Thermal and Reliability Challenges in Chip Components for Automotive High-Performance Compute Systems"*, taught by Dr. Fen Chen of Cruise LLS.
- *"Fundamentals and Applications of Machine Learning in Thermal Management and Heat Transfer Technologies"*, taught by Professor Van P. Carey of UC Berkeley and Professor Alanna Cooney of San Francisco State University.
- *"Passive Two-Phase Cooling: Pulsating Heat Pipes and Loop Thermosyphon"*, taught by Dr. John R. Thome of JJ Cooling Innovation.
- *"Thermal Challenges and Opportunities of Advanced Packages and Microelectronics Systems. Figure of Merit and Applications"*, taught by Dr. Victor Chiriac of Global Cooling Technology Group and Alex Ockfen of Meta.

Navid Kazem

Dr. Navid Kazem is CEO and co-founder of Arieca Inc. He completed his PhD in computational mechanics at Carnegie Mellon where he developed the core technology behind Liquid Metal Embedded Elastomers (LMEE). He is a former Swartz Center for Entrepreneurship Fellow at Tepper School of Business, with multiple high-impact publications and patents. His background combines a deep technical expertise with the capacity to convert cutting-edge scientific advancement into commercial technology. As a CEO with deep technical expertise at Arieca, Navid leads product development of LMEEs, commercial strategic partnerships, as well as fund raising, and is currently serving as program chair of the SEMI-THERM conference.

Dr. Lieven Vervecken

Dr. Vervecken is the CEO and co-founder of Diabatix, a software company specialized in advanced thermal design. Prior to founding Diabatix, Dr. Vervecken received a Ph.D. in mechanical engineering from the renowned KU Leuven in the field of numerical simulations. Dr. Vervecken incorporated his expertise into the advanced A.I. technology at the heart of Diabatix. What started as a small venture has become a fast-growing SaaS company serving multinationals worldwide. Dr. Vervecken is the lead author of multiple peer-reviewed journal articles and an experienced keynote speaker at national and international conferences.

Alex Ockfen, P.E.

Alex Ockfen is a product design engineer at Meta (formerly Facebook), providing technical leadership for thermal and structural design of consumer electronics products. He held previous positions at Raytheon where he obtained experience in thermal management and electronics cooling of a wide range of aerospace and defense applications. He has more than 10 journal and conference publications, is an inventor on multiple patents, is a professional mechanical engineer, and served as the program chair for SEMI-THERM in 2024.

- *"Direct to Chip Liquid Cooling: Single Phase Water and Two-Phase Refrigerant Cooling with Pumped and Passive Systems"*, taught by Professor Alfonso Ortega of Villanova University and Dr. Luca Amalfi of Seguente Inc.
- *"Transient Thermal Analysis Using Linear Superposition"*, taught by Roger Stout, professional engineer retired.

Technical Conference
Held from Tuesday, March 26 to Thursday, March 28, the technical conference featured 26 presentations across seven tracks and eight sessions:
- Consumer Electronics
- Data Center Cooling
- Testing and Measurement Methods
- CFD / Numerical Methods
- Thermal Interface Materials
- Emerging Technologies
- Two Phase Cooling

The technical program also included three invited presentations by industry experts in thermal management:
- Tim Shedd, of Dell, delivered the Keynote presentation on *"Driving Sustainable Scaling of Compute to 2023"*, which explored the key elements of trends, standards, and sustainability in the realm of data centers until 2030 and beyond.
- Wendy Luiten, of WLC, was recognized for winning the SEMI-THERM 40 Thermi Award. Her presentation *"Electronics Cooling Design and Modelling 1984 - 2024"* gave her perspective on her thermal engineering journey (so far).
- Ross Wilcoxon, of Collins Aerospace, presented *"Apollo: The Dawn of Semiconductor Thermal Management"* during a special session on the fourth day of the event.

Awards and Recognition
Bonnie Crystall and Walter Schuch were recognized for winning the SEMI-THERM 40 Hall of Fame Award. Bonnie and Walter, along with Bernie Siegal, laid the foundation for SEMI-THERM in 1984 as its founders. In her speech, Bonnie fondly recalled the early days of SEMI-THERM and expressed gratitude for its growth over the past 40 years. She highlighted the importance of community and collaboration in advancing thermal management.

The Best Paper Award was given to "Simulation of Solder Fatigue Effects on Typical BGA Package due to Material and Temperature Variations" by Jim Petroski of Design by Analysis Technical Consulting

Other technical papers recognized included:
- "Investigation of Flow Restrictors for Rack Level Two-Phase Cooling under Nonuniform Heating" by Serdar Ozguc, Qingyang Wang, Akshith Narayanan, and Richard W. Bonner III of Accelsius,
- "A Thermal Performance Characterization Method for Thin Vapor Chambers by Photonics Technologies", by Kuang-Yu Hsu, Wei-Keng Lin, Yi-Jing Chu, Ming-Hsien Hsaio, and Chiao-Jung Tien of T-Global Technology Co. This paper has been adapted as an article in this issue of *Electronics Cooling Magazine*.

The Harvey Rosten Award, which is sponsored by Siemens Digital Industries Software, is presented at SEMI-THERM. This year's winner was *"Applicability of JESD51-14 to clip-bonded, Discrete Power Devices"*, Szilárd Zsigmond Szőke and Henrik Sebők. The paper was presented at the 2023 29th International Workshop on Thermal Investigations of ICs and Systems (THERMINIC).

Vendor Exhibits and Workshops
Thirty-eight companies participated, showcasing a variety of thermal management products and services, including heat sinks, thermal interface materials, heat pipes, vapor chambers, fluid connectors, air-movers, and advanced materials. Other exhibitors featured tools for thermal simulation and testing, thermal consulting, a university consortium and, of course, *Electronics Cooling Magazine*. In addition to the booths in the exhibit hall, several vendors also gave Vendor Workshops in which they provided detailed information on their products in a more formal presentation format.

Other SEMI-THERM 40 activities included:
- In the panel discussion *"Artificial Intelligence and its Implications for Thermal Engineers; Driving the Thermal Demand"* invited speakers provided their thoughts on the role of AI for thermal engineers. The panel was moderated by Navid Kazem (Arieca) and included Padam Jain (NVIDIA), Kyle Arrington (Intel), Nader Nikfar (Qualcomm) and Tim Shedd (Dell) as panelists.
- In the follow-up panel discussion *"Artificial Intelligence and its Implications for Thermal Engineers; Providing, Using, and*

Powering New Design Tools" invited speakers continued the discussion on the role of AI for thermal engineers. The panel was moderated by Alex Ockfen (Meta) and included Lieven Vervecken (Diabatix), Professor Van Carey (UC Berkeley), Cheng Chen (Meta) and Mehdi Abarham (Ansys) as panelists.

- Invited speakers gave informational and entertaining luncheon presentations on the first two days of the Symposium. On Tuesday March 26, Ken Joyce, independent executive advisor to Brewer Science, Inc., focused on key economic and commercial considerations on domestic packing and test in his presentation entitled *"U.S. Domestic Packaging and Test – The Difficulty and the Opportunity"*. On Wednesday March 27, Sarah da Silva Andrade, Marketing Engineer of Diabatix, talked about the role of social media in promoting scientific research and the importance of digital communication.

About SEMI-THERM

SEMI-THERM, or the Semiconductor Thermal Measurement, Modeling, and Management Symposium, is an annual international conference dedicated to the thermal management and characterization of electronic components and systems. The first SEMI-THERM was held in Phoenix, AZ in 1984 with a goal of fostering networking opportunities for industry and academic professionals in semiconductor thermal management. Over the past decades, the event has developed into its own unique format with technical sessions covering a wide array of topics, from thermal design and modeling to system-level validation testing, providing insights from both academic research and private sector R&D. Additionally, the event includes vendor exhibits where companies showcase their latest products and services in thermal management.

In parallel, the SEMI-THERM Educational Foundation (STEF) was established in 2013 as a Non-Profit Educational Foundation. STEF is dedicated to worldwide educational opportunities and resources within the electronics thermal engineering community, with a goal of providing programs for on-going professional development, technical networking, and engagement of academia and industry in pursuit of innovation and excellence.

More information on SEMI-THERM is available on **https://semi-therm.org/**. SEMI-THERM 41 will be held in San Jose, CA, March 10-14, 2025.

Thermocouple Transient Behavior

Ross Wilcoxon
Associate Technical Editor for *Electronics Cooling*
Collins Aerospace

Previous articles in this series described how thermocouple wire size [1] and thermocouple attachment method [2] can affect steady state temperature measurements. This article briefly discusses how these factors can affect the transient response of thermocouples when used to monitor temperatures that change value over time.

Bare Thermocouple Junction

Before addressing how the thermocouple attachment method affects its transient behavior, it is worth discussing the transient behavior of the thermocouple itself. As described in previous articles, a thermocouple is a welded junction between dissimilar metals that generate a small voltage that is dependent on the temperature of that junction. The welded connection is typically a spherical bead comprised of a mixture of the two metals. This bead is generally small enough that it can be assumed to be fairly uniform in temperature.

The transient thermal response of any mass that is assumed to be uniform in temperature[1] can be described in terms of a time constant, τ, where the transient change in temperature of the mass from its starting temperature, ΔT, normalized by the total possible change that the mass will see, ΔT_{total}, can be written as shown in *Equation 1*:

$$\frac{\Delta T}{\Delta T_{total}} = 1 - e^{-t/\tau} \qquad (1)$$

If the mass is moved from ice water to boiling water, which corresponds to a 100°C temperature change, it would be 63.2°C after one time constant (63.2°C = 100°C*(1-e^{-1}) and 95°C after three time constants.

The thermal time constant of a mass, m, that has uniform temperature at any point in time and has a constant thermal resistance, R, to an external temperature is τ = mcR, where c is the specific heat of the mass. One can estimate the thermal time constant of a thermocouple bead of diameter, D, by considering its mass (m = $\rho\pi D^3/6$), where ρ is the density, and its thermal resistance, R = 1/hA, where the surface area of the bead is πD^2. For a sphere that is small enough that it remains close to uniform temperature, the time constant is shown in *Equation 2*.

$$\tau = mcR = \frac{mc}{hA} = \frac{V\rho c}{hA} = \frac{\frac{\pi}{6}D^3\rho c}{h\pi D^2} = \frac{\rho c D}{6h} \qquad (2)$$

The junction of a type T thermocouple is essentially copper, so its density is 8.9 g/cm^3 and its specific heat is 0.39 J/gK (ρc = 3.47 J/cm^{3}K). A 1mm (0.1cm) diameter thermocouple bead in free convection (with h=10W/m^{2}K =0.001W/cm^{2}K) would have a time constant of 58 seconds. In comparison, a smaller thermocouple with 0.25mm diameter in forced air cooling with convection of 100 W/m^{2}K would have a theoretical time constant of 1.4 seconds.

In practice, the thermocouple wires will add mass (that can increase the time constant) and heat transfer area (that can decrease the time constant). To assess the impact of the wire, a simple finite element model (FEM) of a type T thermocouple was created. 2 cm long 30 gauge wires with a 1mm bead were subjected to convection at 100°C after starting at 0°C. *Figure 1* shows the model at the end of the 300 second simulation.

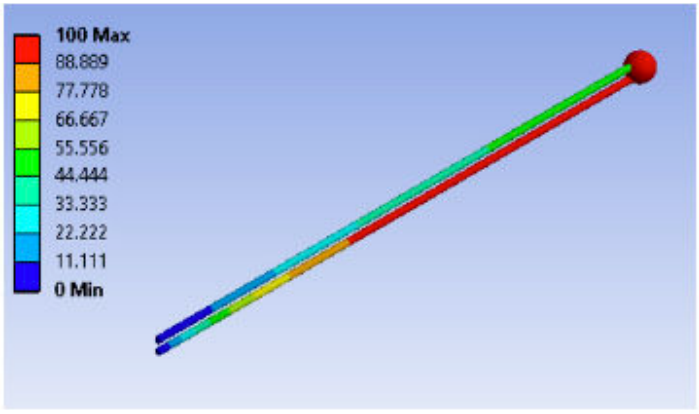

Figure 1: Simple thermocouple model for transient analysis

[1] One can assess this assumption by calculating the Biot number for the mass (Bi = hL/km where h is the convection coefficient, L is the characteristic length (L = D for a sphere) and k is the thermal conductivity of the mass. We can assume that the temperature of the body is approximately uniform at any given time, i.e. it is a lumped mass, if Bi<0.1 [3]

Two levels of convection were applied: 10 and 100 W/m^{2}K; *Figure 2* shows the results from each simulation are compared to the analytical solution of *Equation 2*. This shows indicates that the analytical estimate for thermocouple time constant, using only the mass of the bead, is very close to the FEM analysis. As expected, the thermocouple responds more quickly to the external temperature change with better cooling (higher convection coefficient). However, the small difference between the analytical and FEM solutions is somewhat more noticeable with the higher convection coefficient. The FEM analysis slightly slows the response, presumably due to a larger portion of the wires being affected by the improved cooling.

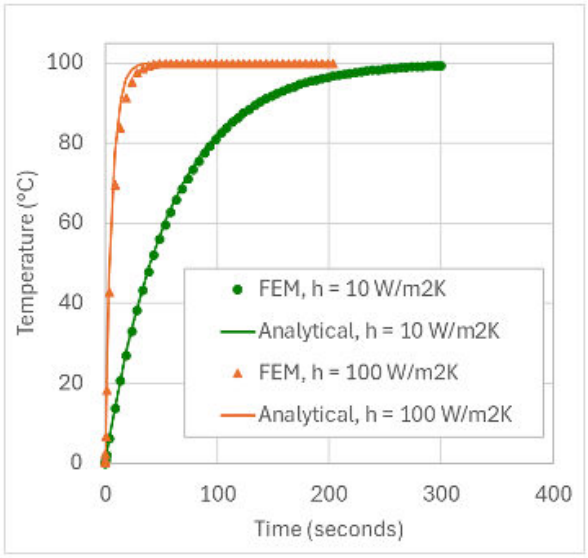

Figure 2: Transient response of a thermocouple with different cooling conditions: comparison between FEM and analytical solutions

Attached Thermocouple Junction

A previous article in this series discussed the effect of thermocouple attachment on steady-state temperature measurements [2]. That testing also revealed some information on how the attachment method can affect its transient response.

Figure 3 shows images of the test fixture and different methods for attaching thermocouples to an aluminum plate. These methods included a) two-part epoxy used in a standard approach, b) a soft tape, c) a quick curing adhesive, i.e. 'superglue'), and d) the same epoxy as used for a) but applied with a dam (a large paperclip) to create a 1mm thick bondline. The aluminum plate was attached to a thermoelectric cooler (TEC) that are maintained at controlled temperatures.

Sixteen thermocouples were attached to the aluminum plate (four replicates for each of the four attachment methods). For the transient testing, the test plate was covered with foam to minimize thermal loss from its top surface. The TEC was set to maintain a temperature of 35°C and allowed to stabilize. The TEC setpoint temperature was then changed to 75°C and the transient temperature response was recorded. The TEC and aluminum plate required approximately five minutes to reach the new setpoint temperature.

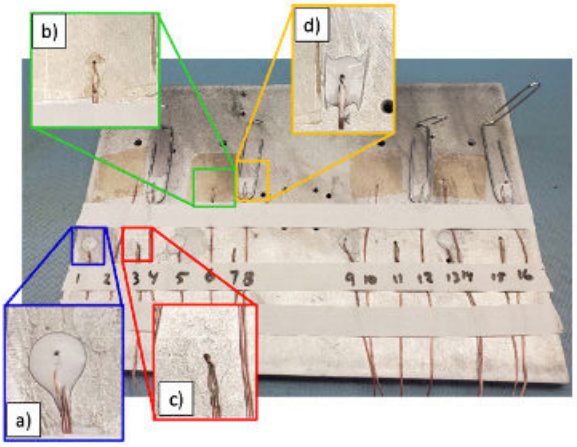

Figure 3: Test fixture for different thermocouple attachment methods

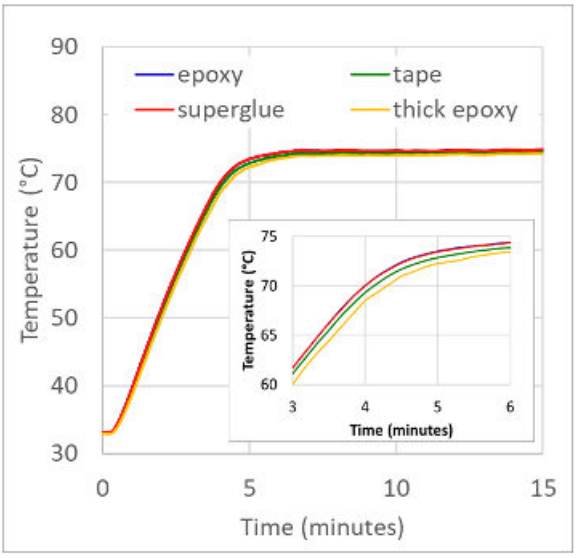

Figure 4: Transient responses of thermocouples when TEC temperature changed by 40°C

Figure 4 shows the average temperature for each thermocouple attachment method and includes a higher resolution image at the 'knee' of interest. This shows that the thermocouples with the different attachment methods had fairly similar transient responses.

However, there are small, but noticeable, differences between the lines in *Figure 4*. These differences are illustrated more clearly in *Figure 5*, which shows the difference between the average temperature for three of the attachment methods relative to the standard method with epoxy.

This plot shows that the transient response with the superglue attachment was nearly identical to the epoxy. However, the other two methods did introduce a small thermal lag that led to a temperature difference between them and the epoxy attachment for a few minutes. Since the responses in *Figure 5* are relative to the thin epoxy data, any attachment method that introduces a larger thermal resistance should lead to a slower transient response. How-

ever, the thick epoxy does have an unexpectedly larger influence on the transient behavior if one only considers the thermal resistance, given that the resistance for the thick epoxy should still be smaller than the thermal resistance to external cooling air[2], which had a time constant on the order of seconds.

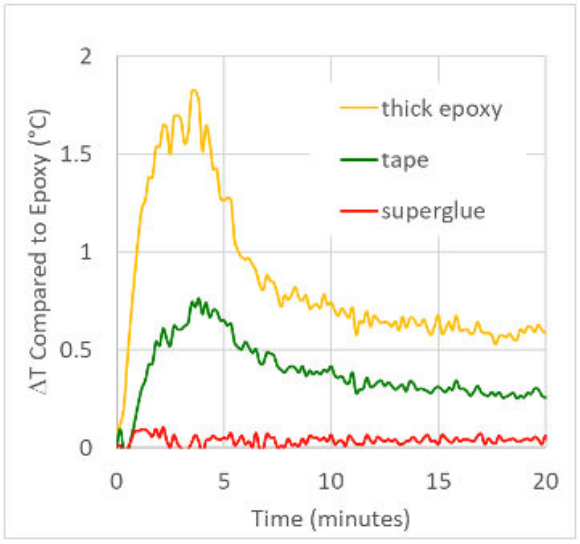

Figure 5: Transient temperature differences of thermocouple attachment method

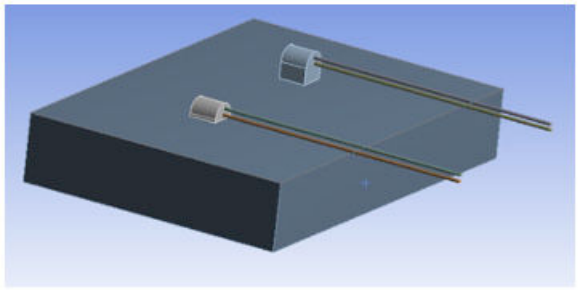

Figure 6: FEM model with two thermocouples on a plate with epoxy attachment - one epoxy attachment is 1mm thicker

One explanation for transient response with thick epoxy is that the epoxy itself has thermal mass and specific heat. While the resistance may be lower, the thick epoxy represents additional mass that must change temperature along with the thermocouple. To assess this, the FEM model was modified to add an aluminum plate and primitive bodies to represent epoxy. *Figure 6* shows an image of the model.

The model was run with the temperature at the bottom of the plate changing by 40°C over a five minute period, which is similar to the experimental transient test conditions. Average temperatures of the thermocouple beads as a function of time are shown in *Figure 7*, which includes an insert that plots the difference in temperature of the two beads as a function of time. The vertical magnitude of the 'bump' in temperature difference in the insert plot is similar to what was experimentally measured.

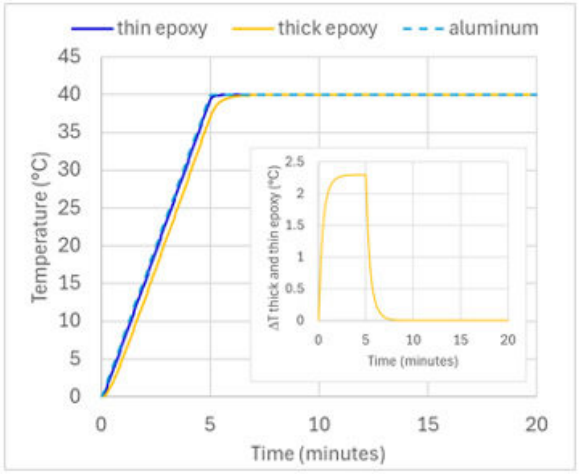

Figure 7: FEM results for two thermocouples with transient heating of plate

Summary

The analytical solution for the transient response of a thermocouple shows that its time constant is proportional to its diameter and the thermal resistance between the thermocouple bead and the object whose temperature is being measured. A simple finite element model confirmed the reasonableness of the analytical solution and that the time constant of a small thermocouple in air will have a time constant on the order of a few seconds at most, depending on the convection coefficient.

When a thermocouple is attached to a surface, even a poor attachment method will have a lower thermal resistance to the object being measured than the same thermocouple being convectively cooled. Therefore, the attachment method generally would not be expected to have a significant effect on the transient response for a step change in temperature. However, the attachment material can add mass to the thermocouple bead and potentially increase its thermal time constant, which reduces its transient response.

References

[1] R. Wilcoxon, "Tech Brief - Thermocouple Size Effects", *Electronics Cooling Magazine*, Spring 2024 Issue

[2] R. Wilcoxon, "Tech Brief - Thermocouple Attachment Effects", *Electronics Cooling Magazine*, Summer 2024 Issue

[3] F.M White, (1984) "Heat Transfer", Addison-Wesley, pp. 163

[2] For example, assuming the epoxy has thermal conductivity of 0.25W/mK, is 1mm thick and the conduction path between the thermocouple bead is a 1mm diameter circle, the conductive thermal resistance is L/kA = 16000K/W, which is ~10% the convective resistance of a 1mm bead in air with convection coefficient of 100 W/m^{2}K

The Critical Radius in Cylindrical Systems

James Petroski
Principal Consultant, Design by Analysis Technical Consulting

In the current world of heat transfer analysis, most work is performed with numerical simulation. However, there are analysis methods, which are faster and useful for early estimates or even design guidance, that are beneficial to thermal engineers. A recent ECM article [1] mentioned the concept of the critical radius when discussing the cooling/insulating effect of wire insulation; this is one of those useful analysis methods that thermal engineers should know about. Critical radius is rarely discussed today and many of the standard heat transfer texts do not mention it, even in passing. This author's modest heat transfer library contains no books with references to the critical radius concept–even the thorough Heat Transfer Handbook from Wiley does not mention critical radius in its voluminous 1,500 pages. The author was taught this concept in his undergraduate heat transfer class at Georgia Tech and this article is a similar introduction to the subject, derived from the class notes [2].

Figure 1 shows the basics of the cylindrical heat transfer case in cross section. While this is often used to examine wire insulation diameters and how to reduce wire temperatures from resistive heating, the concept applies to any similar object with two materials at different distances from the center (not only cylindrical but also spherical), and some method of heat transfer from the outer surface. In theory, other shapes can also be developed but the concept of the critical radius is the one found in older literature with circular cross sections. In this article, the inner region with radius r_1 is the heat generating section. The outer region between r_1 and r_2 is the added, or outer, layer. Heat transfer from the outer layer is a convection loss with a convective coefficient of h_c. Note that different correlations could be used for the coefficient: for wiring, natural convection is most common, but in some environments, such as with fans moving air, a forced air convection coefficient might be appropriate. Radiation may also be included if the temperature difference from r_2 to ambient is significant. The two thermal resistances of conduction through the outer region and convection from the outer surface are represented by Rth(cond) and Rth(conv) respectively.

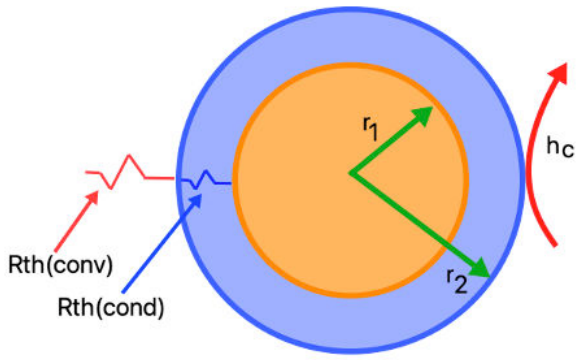

Figure 1: Heat transfer from an insulated cylinder: definition of terms

Before writing the equations and finding the analytical solution, the reader should note that changing r_1 and r_2 influences the thermal resistances in opposite directions. Holding r_1 constant for a moment, as r_2 increases the value of Rth(cond) increases as the heat must conduct a longer distance through more material. However, as r_2 increases, the surface area of the outer region for convective heat dissipation also increases, which reduces Rth(-conv). When these two resistances move in opposite directions, it becomes one of the maximum/minimum problems (optimization) seen in calculus courses.

Changing r_1's value and holding r_2 constant produces a different observation. As r_1 approaches r_2, the conductive thermal resistance of the outer layer shrinks and the heat transfer at the r_2

James Petroski
James Petroski is the owner of Design by Analysis Technical Consulting LLC. He has worked in the area of electronics packaging for nearly 40 years and has a special focus on thermal and mechanical engineering of packages and electronic systems. His background includes equipment design for naval nuclear propulsion instrumentation and controls, NASA space flight experiments (with three shuttle flights of space hardware), computer systems/enclosures, handheld commercial and industrial products, graphite thermal materials and applications, LED lighting systems, and packaging of die and die/substrate systems. He received his Bachelor's in Engineering Science and Mechanics from Georgia Institute of Technology (Georgia Tech) and an MS degree in Engineering Mechanics from Cleveland State University.

boundary remains the same. This means the heat transfer is maximized. However, in critical radius problems, r_1 is usually fixed, so this situation is not typically encountered. Thus, r_1 is normally considered fixed in these problems because wire size or other cylindrical heat source size is fixed.

Detailing the variable r_2 situation in equations, results in the following: R_t heat transfer resistance is the sum of the two parts shown in *Equation 1*, namely

$$R_t = Rth(cond) + Rth(conv) \quad (1)$$

and when the thermal resistances are inserted in terms of the one-dimensional heat transfer equations, this becomes *Equation 2*:

$$Rt = \frac{1}{2\pi k_2 L} ln\left(\frac{r_2}{r_1}\right) + \frac{1}{h_c A_2} \quad (2)$$

where k_2 is the thermal conductivity of the outer region. The terms L and A_2 describe this as a 3D problem where a cylinder of length L is in view and A_2 is the outer area of the cylinder at r_2. This third dimension will cancel out shortly in the derivation of the critical radius. Further, this equation shows the total thermal resistance is also a function of the thermal conductivity k_2. The entire thermal path depends on the thickness of the outer region, its thermal conductivity, and the heat transfer coefficient from the r_2 surface.

The optimization problem can now be created and solved. First, we need to meet the condition (*Equation 3*)

$$\frac{dq}{dr_2} = 0 \quad (3)$$

where q is the applied power. For the critical radius, the optimization is a maximum heat flow rate or a minimum total thermal resistance for the geometry parameter r_2. Using the equation for total thermal resistance, the expression for q (*Equation 4*) is

$$q = \frac{1}{\left(\frac{1}{2\pi k_2 L} ln\frac{r_2}{r_1} + \frac{1}{h_c A_2}\right)} (t_1 - t_{amb}) \quad (4)$$

where t_1 is the internal cylinder temperature (at r_1) and t_{amb} is the ambient temperature. Inserting *Equation 4* into the *Equation 3* condition results in:

$$-\left[\frac{1}{2\pi k_2 L} * \frac{1}{r_2} - \frac{1}{h_c 2\pi {r_2}^2 L}\right] = 0 \quad (5)$$

Solving this for r_2, we find the critical radius to be (*Equation 6*):

$$(r_2)_{critical} = \frac{k_2}{h_c} \quad (6)$$

Thus, the ratio of the outer layer's thermal conductivity to the outer surface's heat transfer coefficient determines the critical radius, at which the heat flow is a maximum in the system. If the system's outer radius is already larger than the critical radius, then any added thickness will impede heat transfer and increase the inner section's temperature.

This result is for a cylindrical system, but it is also possible to generalize this to add a planer and spherical system shown in *Equation 7*:

$$(r_2)_{critical} = (n-1)\frac{k_2}{h_c} \quad (7)$$

where n=1 for a planer wall
(i.e., no critical radius but only added insulation)
n=2 for a cylinder
n=3 for a sphere (derived similarly to cylindrical case)

This formula is helpful for quickly evaluating any cylindrical or spherical system for the thermal impact of changes in radii, changes in thermal conductivity, or changes due to a different heat transfer method (changing h_c). These allow an engineer to quickly assess a possible design change, when tuning a design, without resorting to a longer FEA/CFD analysis.

Where can this be applied? Wire and wire insulation is one area where this can help. A larger wire insulation diameter might be helpful to remove Joule heating in the wires. Other applications can be found on PCBs with conformal coatings applied. Large flat integrated circuits will likely have added thermal resistance since they are planer when compared to their heights. However discrete cylindrical components, such as electrolytic capacitors, can remove heat more effectively with a conformal coating. This is advantageous if these are in a power supply and see higher duty cycles and temperatures. This is counterintuitive for many people but, by demonstrating this with the equations developed here (and shown by testing), the thermal design of a system can be enhanced.

The author is grateful to the late Dr. S. Peter Kezios who taught this and other heat transfer concepts in his Transport Phenomena I class at Georgia Tech in 1980. Dr. Kezios was also a past president of the ASME in the late 1970s. This article is dedicated to him for his work teaching future engineers about sound fundamentals, and for which I am thankful.

References

[1] Wilcoxon, R., Effect of Thermocouple Size, *Electronics Cooling Magazine*, Spring 2024, pp. 9-11
[2] Kezios, S. Peter, Transport Phenomena I, School of Mechanical Engineering, Georgia Institute of Technology, Atlanta GA, 1979 (class notes, published by Georgia Tech)

A Non-Contact Measurement Method for Thin Vapor Chambers by Photonics Technologies

Kuang-Yu Hsu, PhD
Project VP, T-Global Technology

Introduction

In recent years, integrated circuit chips have enabled increasingly powerful computing capabilities as advanced process nodes have moved from DUV (deep ultra-violet) to EUV (extreme ultra-violet) lithography, allowing for higher fabrication resolution and transistor density. Additionally, advanced multi-die packaging has seen increased market demand. As a result, the total thermal power as well as the thermal power density of systems are increasing, leading to the use of a heat spreader such as a metal plate or graphite sheet with good lateral thermal conductivity to relieve the thermal power density. Comparatively, the two-phase vapor chamber (VC) is an even more effective heat spreader in the lateral direction. The structure of a vapor chamber consists of a bottom plate (evaporator) and a top plate (condenser), both made of copper. In between, there are wick structures made of copper mesh and copper powders that contain a small amount of water. After the edges around the plates are sealed, the inner chamber is filled with water (the working fluid), and a vacuum is created inside the device. Other common combinations of VC material and working fluid include titanium/water and aluminum/acetone. When the bottom plate is heated, the liquid in its wick structure evaporates and the phase change absorbs a large amount of latent heat. The heat is then carried away by convection of the vapor. When the vapor reaches the cooler top plate, it condenses back to liquid form, releasing the latent heat. The liquid then returns to the bottom plate by the capillary effect of the wick structure. Vapor chambers are an effective heat spreader because of their ability to absorb large amounts of latent heat during phase change, as well as their effective and uniform spreading of heat via the convection of vapor. Thin vapor chambers, with thicknesses less than 1 mm, are typically utilized in passive cooling designs where available space is very limited. This article discusses measurement challenges regarding thin vapor chambers.

Performance Measurement of Thin Vapor Chambers

Traditionally, contact measurement has been used to measure VC performance. This method often involves the use of resistive rods/wires and ceramic heaters, with a copper block typically inserted between the heater and the vapor chamber to facilitate heat conduction. The thermal dissipation from the heater, Q_e, can be determined from the electrical power, calculated as the product of current and voltage. The presence of the copper block introduces a temperature differential due to its own thermal resistance along the conduction path between the heater and the evaporator plane of the VC. The thermal capacitance of the copper block also stores energy during transient events. Although the copper block is typically insulated, heat losses due to lateral heat dissipation Q_l from the copper block can be significant [1]. *Figure 1* schematically shows the critical test components, VC sample, and the lateral heat loss path in a test setup that relies on contact measurements.

Kuang-Yu Hsu, PhD
Dr. Hsu has worked in the fiber-optics and bio-photonics industries for years. He co-founded a start-up company AcuSolutions Inc. in 2017 dedicated to the development of novel optical section technologies for clinical pathology applications. He was a visiting scholar at Kyoto University in Kyoto, Japan from 2018 to 2020. Since 2022, he has been developing thermal measurement methods using photonics technologies at T-Global. Dr. Hsu holds a BS in Electrical Engineering, and a PhD in Photonics and Optoelectronics Engineering from National Taiwan University. Dr. Hsu has published more than twenty scientific papers and holds twelve U.S. patents.

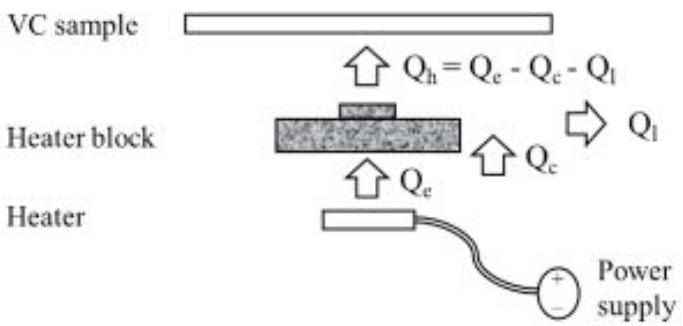

Figure 1: Schematic diagram of the heat losses in a contact measurement system. Q_h: the actual heat load of VC sample

The heater design of commercial test equipment must also consider mechanical attachment for production line applications, which can make the design process even more complex. The temperature gradients due to thermal resistance and lateral spreading, as well as transient effects related to the thermal capacitance of test components, fundamentally limit the amount of heat that can be delivered to the DUT (device under test). The VC's performance is dependent on the heat load since the amount of water in the VC is limited and the temperature uniformity of the VC cannot be sustained beyond a certain power level. An over-estimated thermal load may result in inaccurate OQC (outgoing quality control) and pose potential risks to the final system, making an accurate power estimate particularly important for VC testing. Thin vapor chambers with thicknesses less than 1 mm are typically used in cases when the power is less than 10 W and relative heat losses can be relatively large. Due to the thermal mass of the heater and copper block, contact measurement can also take several minutes to bring the thin vapor chamber up to its correct operating temperature for accurately testing the device. In summary, contact measurement methods are challenging for VC testing due to the required power delivery accuracy and increased cycle time.

A laser heater is an alternative method to precisely deliver thermal dissipation to the vapor chamber by radiation in the form of electromagnetic waves rather than conduction. The thermal conductor (copper block) is no longer necessary and therefore thermal resistance and thermal capacitance issues are eliminated. The directional power flow of electromagnetic waves is described by the Poynting vector $\boldsymbol{S} = \boldsymbol{E} \times \boldsymbol{H}$, i.e., the cross product of the electric field vector $\boldsymbol{E}$ to the magnetic field vector $\boldsymbol{H}$. The output beam from a laser is highly coherent and directional, so the lateral power dissipation is negligible. The power of a collimated laser beam can be directly measured by a high-precision optical power meter. The issue of the accuracy of heat power is solved using the laser heater method [2, 3].

Temperatures at specific locations on the vapor chamber are measured for the test: including T_J at the heated location on the evaporator, T_C on the condenser opposite T_J, and T_X (5.0 cm away from T_C) on the condenser side. The temperature measurement is also non-contact and uses infrared bolometers that detect thermal radiation from objects without contacting the sample. The T_J temperature is important because its position would be in direct contact with the chip. However, when using the infrared bolometer to measure the temperature at T_J, the laser would interfere with the detected signal. Therefore, the Time Domain Extinction Method was used to exclude the laser light from the measurement of T_J. In this method, the temperature is taken when the laser is switched off for a very short interval of time to avoid interference [3]. Using the non-contact method, measurements can be rapidly completed (within 60 seconds) because the temperatures obtained through this process are much closer to thermal equilibrium and much faster than when taken via contact measurement.

Constant Power Measurement

Figure 2 shows the measured results of (a) a vapor chamber and (b) a copper plate using the non-contact method under a power of 5 W. There are some notable differences between the non-con-

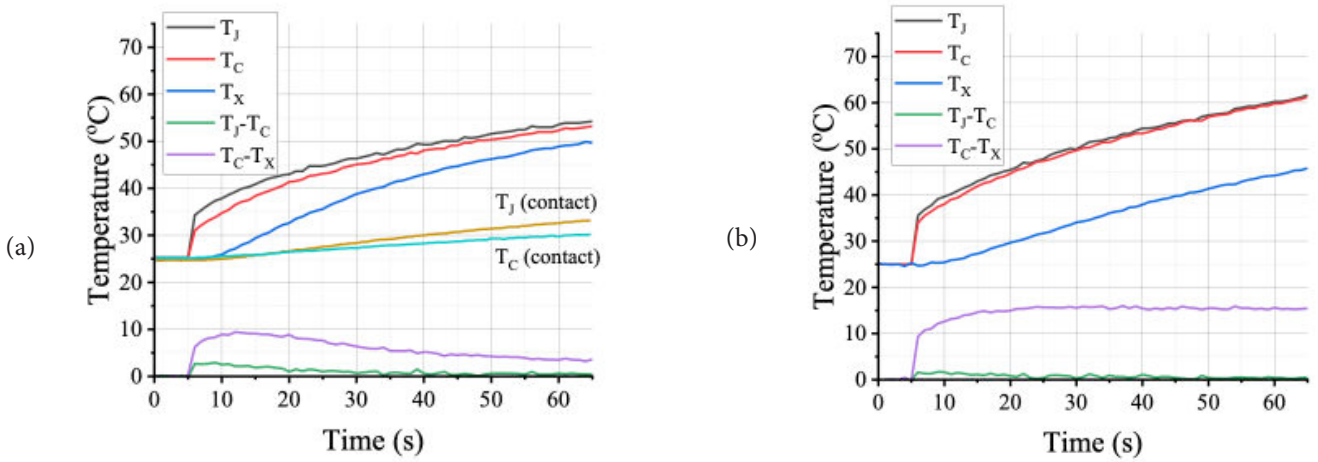

Figure 2: Temperatures T_J, T_C and T_X by non-contact measurement of (a) the vapor chamber (contact measurement results also shown for comparison) and (b) the copper plate. The heat power is 5 W

tact and contact results. First, both the VC and copper plate temperatures increase rapidly with large slopes in the first few seconds after the onset of laser heating, while the temperature curves observed during the contact method have moderate slopes. Additionally, after heating for just 60 seconds, the VC temperatures T_J and T_C reached around 55 to 60°C, which is significantly higher than those reached by the contact measurement over a much longer duration. These results confirm the power delivered to the VC via laser heater is significantly higher than that of a contact heater over the 60-second test duration.

The temperature uniformity, T_C-T_X, is a measure of heat spreading ability. A smaller value indicates the heat effectively spreads over a larger area. Since the heat is less concentrated around the heating spot, T_J decreases. Comparing the VC and the copper plate, T_C-T_X is well within 5°C for the VC, as shown in *Figure 2(a)*, while it is more than 15°C for the copper plate in *Figure 2(b)*. Therefore, the two-phase operating mechanism of a VC is more effective than the thermal conductivity mechanism of a copper plate. T_J of the vapor chamber is 53.9°C and is about 8°C cooler than that of the copper plate.

Regarding power dissipation, since the amount of water in VCs is limited, great care should be taken when using them. When the power goes beyond Q_{max}, the two-phase cycle of liquid water and vapor can no longer be sustained. This is because excess thermal dissipation causes the water in the wick structure around the heater to dry out. For a power of 9 W (higher than Q_{max}), T_C-T_X is greater than 15°C while T_J goes up to as high as 73.1°C, as shown in *Figure 3*.

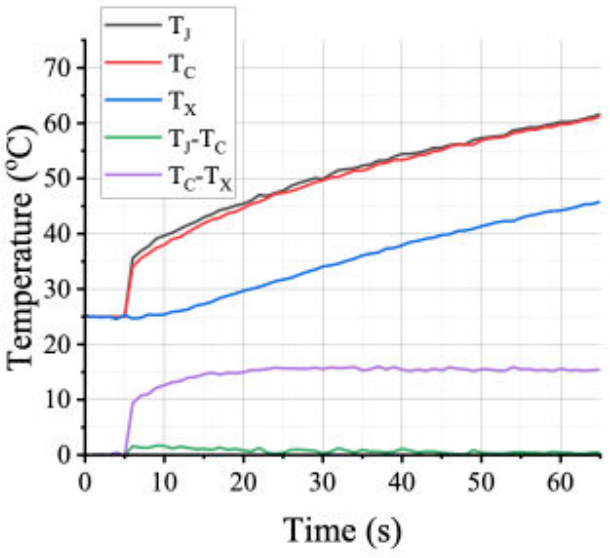

Figure 3: Temperatures T_J, T_C and T_X of the vapor chamber. The heat power is 9 W

Transient-state Measurement

The thermal capacitance in the contact heating method is a limiting factor in transient measurements. The transient response of the vapor chamber was experimentally measured for tens to hundreds of seconds after the onset of heating [4]. The transmission of mobile communication data occurs in bursts, where the transmitted power is boosted for a short period of time, to improve signal to noise ratio and spectrum reuse efficiency, and the thermal dissipation is proportional to transmitted power. Understanding the transient response of the vapor chamber can provide more information to system designers. The semiconductor laser can serve as a function generator of power dissipation by controlling the drive current to generate a variety of profiles, such as a single rectangular pulse. The transient response of the VC can be accurately measured using the laser heating method with a fast response since the thermal capacitance of the copper block is no longer there.

Figure 4 shows a 1-second single rectangular heat pulse generated by the laser. The temperatures of both a VC and a copper plate are measured for comparison, for a dissipation of 10 W, which is greater than Q_{max}. The maximum T_C occurs during the falling edge of the heat pulse. It is 9°C lower for the VC than the copper plate. T_X rises slowly as the heat propagates away from the heated spot. T_X increases faster in the vapor chamber than the copper plate because the heat propagation speed is faster by vapor convection than by copper thermal conduction. The measurements show that the vapor chamber is both a fast-acting and effective heat spreader, which is advantageous for handling transient thermal pulses or spikes. The transient dissipation can go beyond the steady-state Q_{max} limit under the proper power and time duration conditions, as confirmed in *Figure 4*.

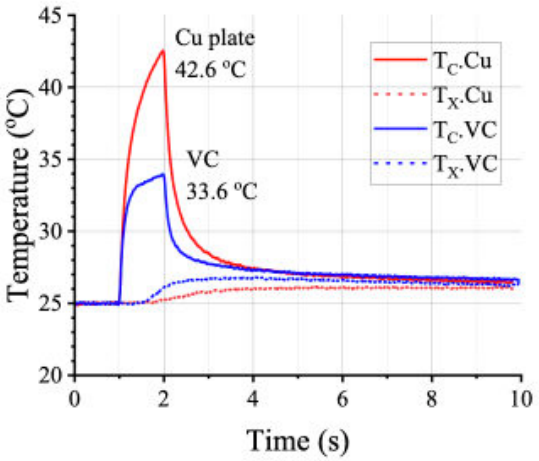

Figure 4: Transient thermal performance of the copper plate and the vapor chamber at 10 W input. The rectangular single heat pulse is shot from 1.0 to 2.0 second

Conclusions

The non-contact measurement method for thin vapor chambers has the advantage of more accurate measurements using the laser heat source, faster measurement time, and the ability to measure transient characteristics. It has great potential for thin vapor chamber testing.

References

[1] G. Patankar, et al., A method for thermal performance characterization of ultrathin vapor chambers cooled by natural convection, *Journal of Electronic Packaging*, vol. 138, 010903, 2016.

[2] X. Jiang, *et al.*, A non-contact thermal testing system for ultra-thin vapor chamber, *Review of Scientific Instruments*, vol. 92, 124902, 2021.

[3] K. Y. Hsu, et al., A Thermal Performance Characterization Method for Thin Vapor Chambers by Photonics Technologies, *40th Semiconductor Thermal Measurement, Modeling & Management Symposium (SEMI-THERM)*, San Jose, CA, USA, pp. 76-82, 2024. https://ieeexplore.ieee.org/document/10535014

[4] G. Patankar, et al., On the transient thermal response of thin vapor chamber heat spreaders: Governing mechanisms and performance relative to metal spreaders, *International Journal of Heat and Mass Transfer*, vol. 136, pp. 995-1005, 2019.

Power Density In the Context of Two-Phase Immersion Cooling

Jimil M. Shah, PhD
Immersion Cooling Staff Engineer, Stealth Startup

Phillip E. Tuma

Abstract

Data centers face challenges in balancing space and power, with studies showing that when power density exceeds 7kW per rack, IT equipment space utilization drops to 50%. Traditional cooling methods are reaching limits due to increasing demands from deep learning and AI, necessitating more space. Two-phase immersion cooling offers simplicity and cost savings compared to traditional methods. Submerging equipment in liquid allows for significant energy savings and accommodates future load densities. This article explores power density from the perspective of two-phase immersion cooling, comparing it with air cooling at higher densities. Two-phase immersion cooling increases floor space density by over six times, simplifying server design and reducing costs. At higher densities, the cost of fluid relative to electronics becomes negligible.

Nomenclature

A_t	Area of a tank opening
L_t	Length of a tank
W_t	Width of a tank
V_{server}	Server chassis volume
L_{server}	Server length
W_{server}	Server width
H_{server}	Server height
ΔH	Liquid level rise in the tank
$V_{displaced}$	Displaced server volume
V_{other}	Displaced volume of air-cooling hardware and steel chassis
$V_{electronics}$	Displaced volume of electronics alone
V_{air}	Volume of air
V_{fluid}	Volume of fluid
m_{fluid}	Mass of fluid
$m_{electronics}$	Mass of electronics
$D_{electronics}$	Power Density of electronics [kW/liter]
P2PIC	Passive two-phase immersion cooling

Jimil M. Shah, PhD
Jimil M. Shah, PhD, is an Immersion Cooling Staff Engineer at a Stealth Startup, spearheading the development of cutting-edge two-phase immersion cooling systems for hyperscale data centers. His work focuses on enhancing energy efficiency and reducing operational costs, particularly in thermal and reliability aspects. Previously, Dr. Shah served as Senior Director of Thermal Sciences at TMGcore, and as an Application Development Engineer for Server Liquid Cooling at 3M Company. His research in advanced cooling solutions for data centers includes direct-to-chip and immersion cooling with dielectric fluids. Dr. Shah received his doctorate in Mechanical Engineering from the University of Texas at Arlington and has numerous patents and publications in the field.

Phillip E. Tuma
Phil Tuma worked for 27 years at 3M Company developing applications for fluorinated heat transfer fluids in various industries including pharmaceuticals, military/aerospace, power electronics, and semiconductor processing. For the past 15 years he has studied the mechanical systems and the physical, organic, and electrochemical processes that enable the use of passive 2-phase immersion for cooling high-power density compute systems. He holds a BA from the University of St. Thomas, a BSME from the University of Minnesota, and a MSME from Arizona State University.

Introduction

Increased power density (the amount of power per unit volume) is often listed among high priorities for data center operators who rightly perceive that higher rack density can drive down data center costs. However, in traditional air-cooled data centers, increased density does not necessarily translate to improved economics [1].

Higher-density servers increase IT capacity per rack, but this can strain fan power and computational efficiency [2]. This rise in IT density can decrease data center footprint but requires sufficient temperature and airflow conditions [3]. Capital costs escalate with the additional plena, filters, and heat exchangers needed for these denser racks. Modern servers utilize multiple fans to direct air toward hot components, increasing power consumption, noise, and the risk of system failures [2]. While modern processor designs distribute work across low-power processors to mitigate heat, air cooling limits potential processor density [3]. Liquid cooling technologies enable a much higher power density. However, direct-to-chip water cooling and even liquid/single-phase immersion cooling eventually reach density levels at which the flow of the coolant becomes an engineering challenge in a manner similar to air-cooling [4-6].

Passive 2-phase immersion cooling (P2PIC) is different in this respect because many aspects of P2PIC improve with density. A certain level of density is a requisite to economically justify this approach, with economics that continues to improve with higher density. To explore how and why this is so, it helps to think of power density not in traditional units like kW/rack or kW/m^2 but to consider it as Archimedes would, by volume displacement.

In this study, the true volume of the electronics and air-cooling hardware in a 2U server is measured in this way, permitting direct calculation of the fluid volume required to cool it by immersion. These data are then used to extrapolate to higher hardware power densities where the advantages of immersion emerge.

Experimental Procedures

Measurement of Power Density by Displacement

Figure 1 (a) shows a tank of liquid and a server chassis. The cross-sectional area of the rectangular tank as seen from above is

$$A_t = L_t W_t \tag{1}$$

The server chassis volume is calculated from its XYZ dimensions as

$$V_{server} = L_{server} W_{server} H_{server} \tag{2}$$

When submerged in the tank of liquid (*Figure 1 (b)*), the server displaces a volume of liquid such that the liquid level in the tank rises by ΔH. The actual *displaced* server volume is then

$$V_{displaced} = A_t \Delta H \tag{3}$$

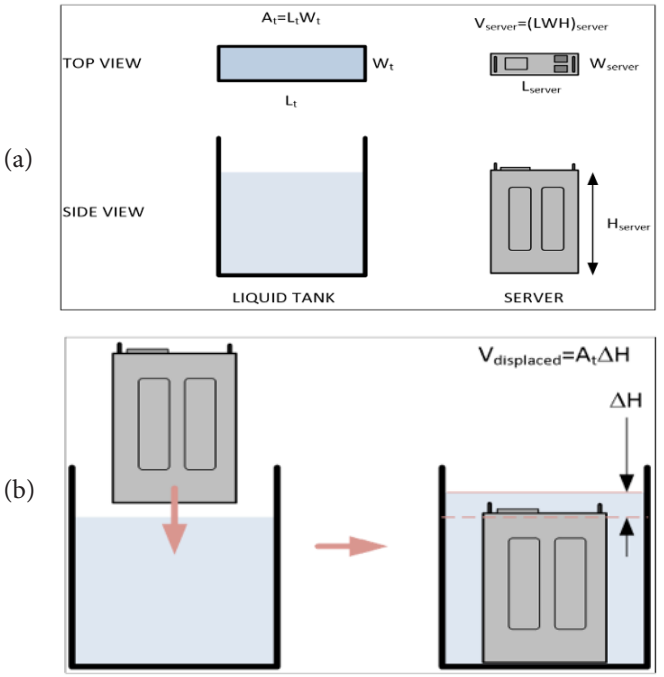

Figure 1: (a) Tank and server and (b) Measurement of server displacement

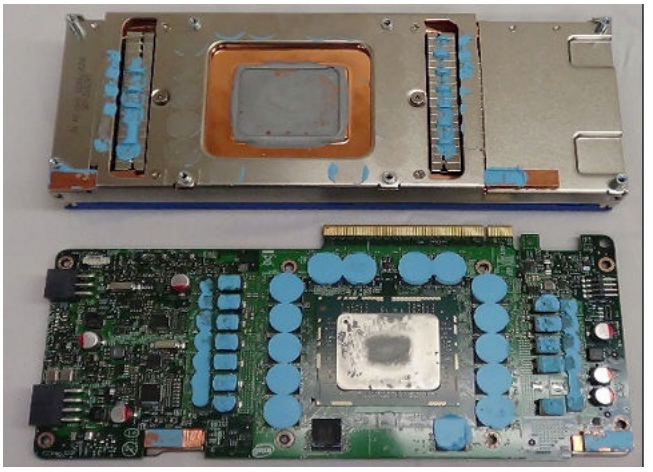

Figure 2 (a): Removal of GPU card from its heatsink

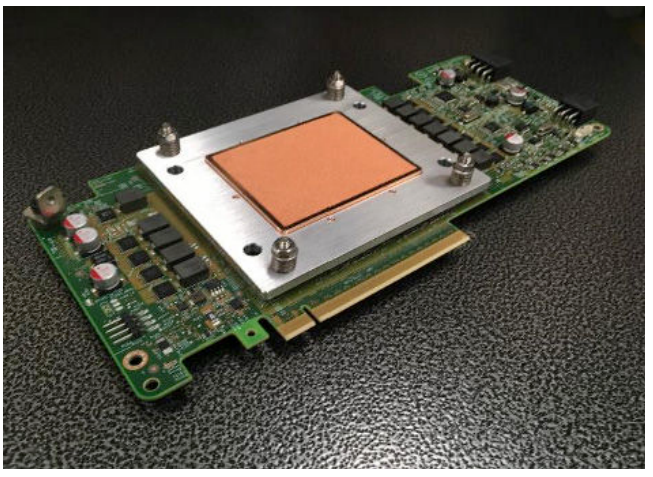

Figure 2 (b): A copper boiler mounted on the GPU

Additional experiments were conducted to isolate the displacement of various components of a server as shown in *Figure 2 (a)*. These were broadly grouped into 2 categories: The first, V_{other}, includes those components that exist purely for air cooling, such as fans, heat sinks, shrouds, ducts, etc. It also includes the steel used to make the chassis and to arrange the electronics within. The second, $V_{electronics}$, includes the rest of the server, those things that would be difficult to dispense with as they ARE the server. These include the PCBs, chips, capacitors, power supplies, etc. that comprise the server. A copper boiler made by Cooler Master (Taiwan) is mounted on an Intel Xeon Phi math coprocessor as shown in *Figure 2 (b)*. Such a boiler is the only additional volume required for 2-phase immersion. The remaining volume is air but also represents the volume that must be filled with liquid if the same server is to be immersion-cooled.

Results and Discussion

The results of these experiments are shown in *Figure 3*. Though the server chassis is 14% solid matter, only 6% of its total volume is occupied by electronics (*Figure 3*). Calculations like these point to the illogicality of immersion cooling servers that were designed to be cooled by air.

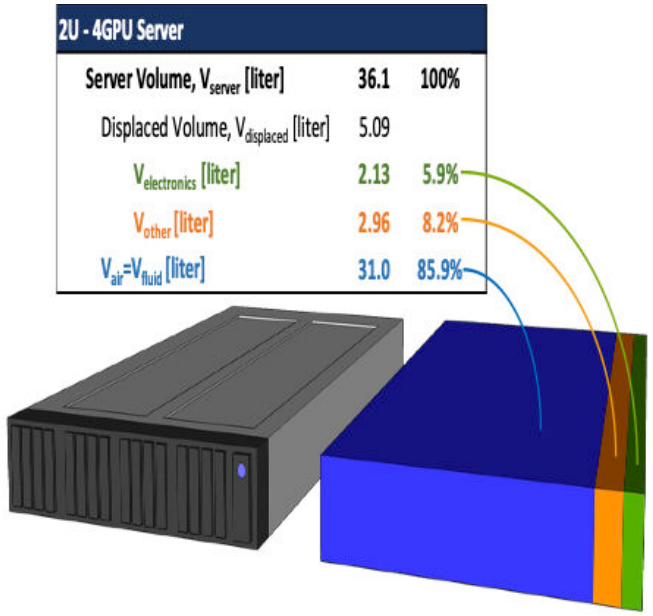

Figure 3: Summary of volume displacements for 2U Server

The 5mm Datacenter

If you could air cool 21 of these servers (27.3 kW) in a conventional rack (23 inches wide x 39 inches deep x 2-meter height), the total volume of the electronics ((21 servers x $V_{electronics}$ = 2.13 liter from *Figure 3* x 1000) cm^3) would represent only 8cm (4%) of the rack's 2-meter height, with the fluid required to fill them reaching another 112cm (*Figure 4*). If the volume of the electronics was instead distributed at a typical data center floor space density of 3kW/m^2, it would be only 5mm thick, a result that belies the use of a multi-story facility that might house it (*Figure 5*).

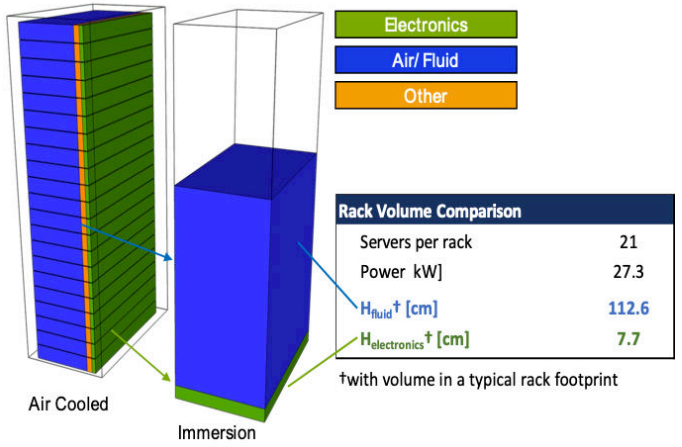

Figure 4: Total volume of fluid required to immersion cool a rack of conventional air-cooled servers compared to the actual volume of the electronics

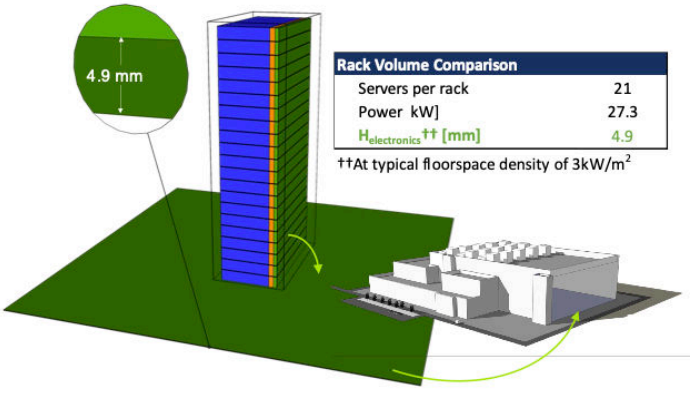

Figure 5: Volume of electronics if spread to a typical data center floor space density of 3kW/m^2 would be only 5mm tall

Extrapolating to Higher Density

These data can be used to extrapolate to higher power density. For this analysis, the volume of the steel chassis (found to be half of the volume of V_{other}) is assumed to remain constant (*Table 1*). The mass of electronics per displaced volume, which averages 4.5 kg/liter, and the electronics power density of $D_{electronics}$=0.61 kW/liter (from the server power and *Figure 3*) are also held constant. A fluorochemical fluid density of 1.6 kg/liter is assumed. The power density, expressed as $V_{electronics}/V_{server}$, is then increased while V_{server} is kept constant.

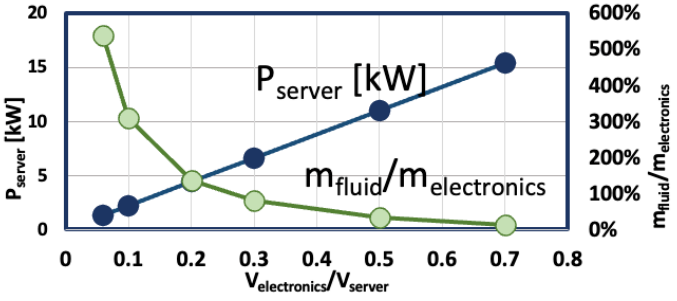

Figure 6: $V_{electronics}/V_{server}$ Vs $m_{fluid}/m_{electronics}$

V_{server} = const = 36.1 liter

$V'_{electronics}/V_{server}$	0.06	0.1	0.2	0.3	0.5	0.7
$V'_{electronics}$ [liter]	2.17	3.61	7.23	10.84	18.07	25.29
V'_{other} [liter] = 0.5 V_{other}	1.48	1.48	1.48	1.48	1.48	1.48
V'_{fluid} [liter]	32.49	31.04	27.43	23.81	16.59	9.36
$V'_{displaced}/V_{server}$	0.10095	0.14095	0.24095	0.34095	0.54095	0.74096
P'_{server} [kW] = $D_{electronics} \times V'_{electronics}$	1.32	2.21	4.41	6.62	11.03	15.44
Fluid Requirement [liter/kW]	24.55	14.08	6.22	3.60	1.50	0.61
$m'_{fluid}/m'_{electronics*}$	533%	305%	135%	78%	33%	13%

* mass density of electronics averages 4.5 kg/liter

Table 1: Extrapolations of 2U calculations to higher density [fluid requirement]

This analysis shows how the mass of fluid becomes less significant relative to the mass of the electronics as the power density increases (*Table 1*). When $V_{electronics}/V_{server}$= 70%, the fluid requirement has dropped from 25 to <1 Liter/kW (*Table 1* and *Figure 6*) and 11 of the 15kW servers can be placed in a 170kW tank with 6 times the floor space density of the air-cooled rack (*Figure 7*).

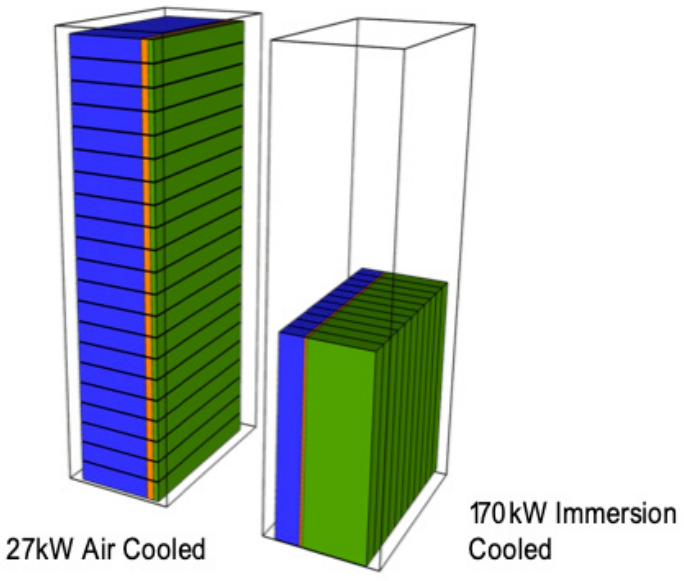

Figure 7: Power output of 21 air-cooled servers in a standard rack compared with 11 hypothetical immersion-cooled servers occupying a standard rack footprint

Reality Check

Will P2PIC even function at this density? One 40MW two-phase immersion facility [6] uses less than 2 liters of fluid per kW with 12kW 1U modules housed in 250kW tanks that use 48-53°C water to cool. These same tanks are sized for up to 500kW to accommodate next-generation hardware. One can look also at the refrigeration industry, in which 2,000+kW low-pressure chillers [7] are deployed with evaporator footprints no larger than these tanks. Lastly, technology demonstrations with simulated computer hardware showed that fluid power densities, $D_{power, fluid}$ <0.1 Liter/kW are possible [8].

Additional Considerations

There are additional savings to be gained at the server level:

- The cost of engineering an air-cooled solution for a modern server can be quite high and involves computational fluid dynamics simulations, wind tunnel testing, and validation.
- A myriad of heat sinks, interface materials, isolation pads, conformal coatings, fans, and baffles can be eliminated from servers and power supplies.

There will, of course, be costs incurred in immersion cooling and these are primarily associated with more rigorous pre-cleaning of hardware, cleaner cabling insulations, and the capital cost of nontraditional test and burn-in equipment for hardware that can no longer be cooled by air.

However, savings at the facility scale can also be realized and most have been demonstrated in the aforementioned 40MW facility of detailed projections:

- Elimination of raised floors, fans, air filters, baffles, plena, adiabatic, or refrigerated cooling equipment coupled with reductions in telecom requirements can reduce facility costs by up to 43% [9].
- Elimination of fire protection equipment would reduce facility costs but will require modification of relevant industry standards. The merits of submerging IT equipment in a clean agent fire suppressant are already recognized [10].
- Ability to re-use tanks and mechanical infrastructure for future generations of hardware.

Simplicity

- Ability to design hardware, to densities that reduce the fluid requirement to <0.1 Liter/kW [8], without regard for how it will be cooled. No airflow simulations, thermal solution validation, etc. needed.
- Passive heat transfer process. No use of rack pumps, redundant pumps, controls, etc.
- Elimination of node-level cooling hardware. No requirements of cold plates, interfaces, manifolds, quick disconnects, hoses, etc.
- Reusable, environmentally sustainable working fluids like Hydrofluoroethers (HFEs), fluoroketones, hydrofluoroolefin (HFOs), etc., which have no Ozone Depletion Potential (ODP) and very low Global Warming Potential (GWP). [14].

Challenges on the Path to x86

- As is always true with any burgeoning technology, challenges to the implementation of two-phase liquid immersion cooling exist; including concerns about fluid loss, fluid selection, material compatibility, safety, and environmental impact. While outside the scope of this work, these must be evaluated for this technology to succeed for a given application.
- The challenges in advancing x86 technology include securing a reliable supply chain for compatible materials, ensuring effective maintenance and fluid loss mitigation, developing an ecosystem that supports high power density, statistically meaningful demonstrations in the realm of x86, and commercially available turn-key systems.
- Given the importance of fluorochemical fluids in two-phase liquid immersion cooling, it's understandable that readers may have concerns about their future availability, especially in light of recent developments at 3M. However, the current state of the market indicates no significant issues with the availability of these fluids. Although this article does not delve into supply chain specifics, it's important to note that the availability of fluorochemical fluids remains stable. Some key suppliers include Unistar Chemicals, Inventec Performance Chemicals, and Chemours. These companies ensure both a reliable supply and alternative options. Of course, testing the viability of these potential alternatives will be crucial.

Conclusion

Though comprised of energy-dense GPU hardware, the volume of the chassis in this study is more than 90% air. The low power density of the air-cooled server hardware intensely affects the economic feasibility of immersion cooling. A modern 1.3kW, 2U GPU server was only 6% electronics on a volumetric basis. The electronics comprising 21 of these servers (27kW, 42U) would fill only the bottom 8cm of a rack footprint. The fluid required to fill them would require an additional 112cm and the fluid mass would be 5X that of the server.

Higher-density hardware, already realized in Bitcoin mining, enables the value proposition of immersion [11,12,13]. If a server could instead be 70% electronics, it would be 15kW, enabling 170kW dissipation to be housed in the footprint of a traditional rack. The fluid required to submerge this hardware would represent around 14% of the electronics' mass.

In a nutshell, a volume displacement analysis reveals just how low the power density in a typical facility is. At 3kW/m^2, a typical air-cooled data center floor space density, the electronics in a typical data center would fill only the bottom 5mm of the building which is often several stories tall. P2PIC can increase floor space density 6 times or more while simplifying server design and reducing facility capital and operating costs. With increased density comes increased interconnect bandwidth and the potential to reduce E-waste.

References

[1] Bob West, 29 Aug 2018, https://www.datacenters.com/news/understanding-the-interplay-between-data-center-power-consumption-data-center-en

[2] Cho J, Park B, Jeong Y. Thermal Performance Evaluation of a Data Center Cooling System under Fault Conditions. Energies. 2019; 12(15):2996. https://doi.org/10.3390/en12152996

[3] Alex Carroll, 13 March 2019, https://lifelinedatacenters.com/data-center/data-center-power-density/

[4] Stansberry, M., "UPTIME INSTITUTE DATA CENTER INDUSTRY SURVEY 2015," Copyright Uptime Institute, 2015.

[5] Brown, K., Torell, W., and Avelar, V., "Choosing the Optimal Data Center Power Density," White Paper 156, Copyright 2014, Schneider Electric, http://www.apc.com/salestools/VAVR-8B3VJQ/VAVR-8B3VJQ_R0_EN.pdf

[6] Anthony Horekens, 12 November 2018, https://www.allied-control.com/publications/Allied-Control-to-Exhibit-Immersion-Cooling-Solutions-with-Orange-Silicon-Valley-at-SC18-Conference.pdf

[7] "Trane® CenTraVac® Chillers", Accessed on 10th April, 2019, CenTraVac meets today's efficiency and sustainability challenges, https://www.trane.com/commercial/north-america/us/en/products-systems/chillers/water-cooled-chillers/centrifugal-liquid-cooled-chillers.html
[8] Tuma, P. E., "The Merits of Open Bath Immersion Cooling of Datacom Equipment," Proc. 26th IEEE Semi-Therm Symposium, Santa Clara, CA, USA, pp. 123-131, Feb. 21-25, 2010.
[9] Tuma, P., et al, "30MW Immersion Cooling Datacenter," Presentation, Datacenter Dynamics 2017 Cloud + Colo, Dallas, TX, Sept. 26, 2017.
[10] Ip, G., et al, "A Novel Way to Maximize Energy Efficiency, Power Density and Fire Protection in Data Centers," Presentation, 2014 SFPE Conference & Expo, Long Beach, Ca, Oct. 12-17, 2014.
[11] Tuma, P., & Shah, J. M., 2020, "Recent Developments in Immersion Cooling with Fluorochemical Fluids by Open Compute Community," May 2020, Open Compute Project Virtual Summit.
[12] Tuma, P., Shah, J. M., & Crandall, T., 2019, "Recent Developments in Computer Immersion Cooling with Fluorochemical Heat Transfer Fluids," SEMI-THERM® Thermal Technologies Workshop, November 4-6, 2019, Microsoft Corporate Conference Center, Redmond WA USA.
[13] Shah, J. M., and Tuma, P., 2022, "Power Density in the Context of Two-Phase Immersion Cooling," ASME Paper No. IPACK2022- 96370. 10.1115/IPACK2022- 96370
[14] Shah, J. M., 2024, "Unlocking Potential: Navigating Challenges and Seizing Opportunities In Two-Phase Liquid Immersion Cooling", Tech Talk, IEEE ITherm 2024, Denver, CO.

Theta-JC Measurements: Steady-State Compared to Transient Methods

Jesse Galloway
Reliability and Thermal Engineer Consultant

Robin Bornoff
Innovation Roadmap Manager, Siemens Digital Industries Software

Thermal characterization plays a vital role in electronic package reliability testing, design, and verification of manufacturing processes. The reliability of electronic packages is controlled, in part, by ensuring the maximum junction temperature is not exceeded during operation. Systems such as cell phones, electric vehicles and computers, must operate with die temperatures below their maximum allowable temperature. A clear definition of thermal metrics used to characterize thermal performance is needed to exchange necessary design information between electronic package manufacturers, system designers and reliability engineers. This study compares steady-state and transient methods used to measure component junction-to-case thermal resistance, Theta-JC. Transient Theta-JC measurements tend to predict lower thermal resistance compared to steady-state Theta-JC measurements when multi-directional heat flow paths are present.

Comparative Metrics Versus Predictive Models

Comparative metrics are used to contrast the performance of one device to another while operating under the same conditions, see for example the thermal metrics developed by the JEDEC JC-15 Thermal Characterization committee [1] and the AQG-324 guideline [2].

Thermal resistance is a metric commonly used as an electrical circuit analog to represent heat flow restrictions in thermal systems. In an electrical environment, a voltage drop occurs when current flows through a trace of a given resistance. Since the electrical resistivity of a typical insulator surrounding a trace is at least 10 orders of magnitude higher than the trace, for all practical purposes, current only flows through traces. In contrast, the thermal resistance of insulators surrounding thermally conducting materials is only perhaps 3 orders higher. Due to lower resistance, heat spreads more readily into thermal insulators than current into electrical insulators. While it is therefore difficult to make the argument of one-dimensional conduction for thermal applications, in the purest sense, thermal resistance is defined as the temperature drop between a hot isothermal plane, T_H, and a cold isothermal plane, T_C, divided by the heat flow, Q, as shown in *Figure 1*. A good overview of the limitations of the thermal resistance

Jesse Galloway
Jesse Galloway received his PhD in Mechanical Engineering in 1991 from Purdue University in West Lafayette, Indiana. His graduate research focus was on experimental and theoretical boiling heat transfer. After graduating, Jesse worked as a thermal engineer at Motorola, Fujitsu and Amkor and most recently as a reliability engineer at onsemi. Currently Jesse is a consultant living in Florida. His work experience includes predicting the reliability of electronic systems, thermal characterization, thermal design of heat sinks and experimental testing. He has published more than 30 conference and journal articles and has been granted 6 patents.

Robin Bornoff
After receiving a bachelor's degree in Mechanical Engineering in 1992 and a PhD for CFD research in 1996 from Brunel University in the UK, Robin joined Flomerics as a Flotherm support and application engineer. By the time of the acquisition of Flomerics by Mentor Graphics in 2008 he was the Product Marketing Manager for Flotherm. Now in Siemens Digital Industries Software, he is an Innovation Roadmap Manager in the Simulation and Test Solutions division. With over 25 years experience in the field of electronics thermal simulation, he has published over 30 journal and conference papers and has had 7 patents granted.

concept is discussed by Lasance [3]. Actual semiconductor packages do not have isothermal planes nor does heat flow in a single direction. Despite these limitations, thermal resistance is still a useful concept in developing a comparative metric to contrast the thermal performance of different packages.

Theta-JC, also written as $\emptyset_{JC}$ or R_{jc}, is a comparative metric used to define the thermal resistance between the die and the semiconductor package case. It is defined by *Equation (1)* where $T_{j,max}$ is the maximum junction temperature, T_C is the outer case surface temperature measured directly above the hot spot on the die and P_c is the power flowing through the case surface.

$$\theta_{JC} = \frac{T_{J,max} - T_C}{P_c} \quad (1)$$

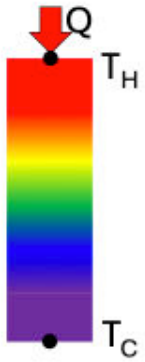

Figure 1: Theoretical definition of thermal resistance

Significant errors may result when comparative metrics, such as Theta-JC, are used as predictive models. It is tempting to rewrite *Equation (1)* to predict $T_{j,max}$ for a different set of application conditions, where P_{tot} is the total dissipative power.

$$T_{j,max} = T_c + \theta_{jc} * P_{tot} \quad (2)$$

The problem with applying *Equation (2)* to predict $T_{j,max}$ is that Theta-JC is measured during characterization tests in which power is only conducted to the case. However, in *Equation (2)*, $T_{j,max}$ estimates are made using the total power flowing in more than one direction as usually happens in operation. Also, when *Equation (2)* is applied to predict $T_{j,max}$ for an application that utilizes a different heat sink design, errors will result due to differing heat flow paths. It is therefore important to use comparative metrics only to compare the performance of one package design to another when considered in the same testing conditions.

Predictive models must consider more than one heat flow direction. Examples of steady-state predictive models include the two-resistor model [4] and the Delphi thermal network model [5]. For the more general transient cases, reduced order models (ROM) [6] or full order models (FOM) may be used to accurately predict junction temperatures for different application environments

Steady-State Thermal Resistance

The first Theta-JC test considered here is based on a steady-state method, see MIL-STD-883E [7]. Electrical power is supplied via a current source to the die and the virtual die temperature is measured by reading a temperature-dependent voltage drop at the die, e.g. for a MOSFET between drain and source, see JESD51-1 [8]. *Figure 2* shows an example of a steady-state Theta-JC test setup for a leaded discrete device.

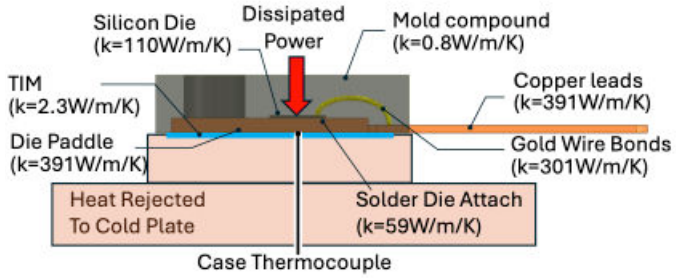

Figure 2: TO247 package steady-state Theta jc test setup

Power that doesn't flow into the case, P_{NC}, includes the heat flowing into the motherboard, power leads or other surfaces, and is not included in the calculation of Theta-JC.

$$P_c = P_{tot} - P_{NC} \quad (3)$$

An estimate for P_{NC} may be made by running the Theta-JC test using the same setup but with the cold plate replaced by an insulating block. P_{tot} is adjusted to produce the same $T_{j,max}$ as measured during the cold plate test. Using a well thermally insulated block, P_c may be approximated as zero and P_{NC} will be approximately equal to P_{tot}. This method may be used to test improvements to thermal insulation and test boards designed to minimize P_{NC}.

Experimental measurement errors in calculating Theta-JC can be reduced by using the temperature differences referenced to a zero-power condition. *Equation (4)* is equivalent to *Equation (1)* since at the zero power condition, $T_{j,max,P=0}$ equals $T_{C,P=0}$.

$$\theta_{JC} = \frac{(T_{j,max,P} - T_{j,max,P=0}) - (T_{C,P} - T_{C,P=0})}{P_c} \quad (4)$$

$$\theta_{JC} = \frac{\Delta T_{j,max} - \Delta T_C}{P_c} \quad (5)$$

Measuring the case temperature is challenging for high power packages, due to the large temperature gradient in the thermal interface material (TIM). Moreover, there are large temperature

gradients across the case surface at a location directly below the die. These spatial temperature variations make it difficult to repeatably measure case temperature with a temperature probe.

Transient Theta-JC Measurement

To overcome the experimental uncertainty in measuring case temperature, a second method called transient dual interface method (TDIM) was developed, see JESD51-14 [9]. TDIM is applicable for packages that exhibit one-dimensional heat flow where P_{NC} is approximately zero and $P_C = P_{tot}$. A transient impedance, defined in *Equation (6)*, tracks changes in junction temperature as a function of time. Note the similarities between *Equations (1)* and *(6)*. A step change in power at times greater than zero is applied and the corresponding junction temperature is measured.

$$Z_{th} = \frac{T_{j,t} - T_{j,t=0}}{P_{tot}} \qquad (6)$$

The time at which the transient thermal wave reaches the case can be determined by testing the same package twice. The first test uses a higher resistance TIM and the second test uses a lower resistance TIM, referred to as dry and wet TIM, respectively. At early times, before the thermal wave reaches the case, Z_{th} follows the same curve for both dry and wet TIMs. Once the thermal wave reaches the case, Z_{th} increases at a greater rate for the dry TIM compared to the wet TIM, as shown in *Figure 3*.

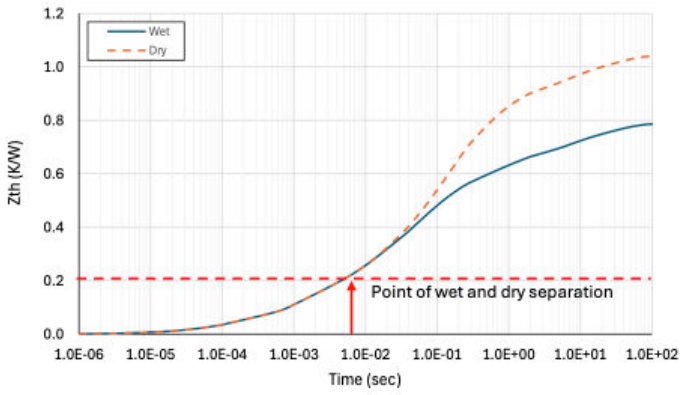

Figure 3: TO247 simulated Z_{th} curve separation

The Z_{th} value at the point of separation of the dry and wet curves may be used to estimate Theta-JC. A more detailed description of this method is given in JESD51-14 [9]. The major requirement for the application of the TDIM Theta-JC measurement is one-dimensional heat flow. This requirement is rather restrictive and typically only applies to die that are mounted to a low-resistance heat spreader with a high-resistance thermal path in the opposite direction. The TO247 and micro lead frame (MLF) are examples of electronic packages that exhibit one-dimensional heat flow. If the heat flow path is multi-dimensional, values of Theta-JC measured by TDIM tend to be lower than Theta-JC measured by the steady-state method.

Experimental Measurements

Experimental Theta-JC measurements were performed on two thermal test vehicles (TTVs) to compare TDIM and steady-state measurements. The first TTV is a flip chip ball grid array (FCBGA) package and the second TTV is a wire bond plastic ball grid array (PBGA) package. Details for each package are listed in *Table 1*. Both package styles experience multi-dimensional conduction, i.e., heat flows both to the case and to the motherboard side of the package. It is known that TDIM Theta-JC values will be lower than steady-state Theta-JC values, see for example Bornoff [10], due to the multi-dimensional heat flow that is not accounted for when using TDIM. TDIM measured Theta-JC is approximately 2X lower than steady-state Theta-JC measurements, as shown in *Table 1* and *Figure 4*. Error bars shown in *Figure 4* represent ± one standard deviation.

Package	FCBGA	PBGA
Body size (mm)	45	35
Die size (mm)	10.0	10.0
Heat spreader size (mm)	40	27
Interconnect style	Flip chip	Wire bond
Steady-state Theta-JC Mean ± Std Dev	0.706 ± 0.033	5.12 ± 0.012
TDIM Theta-JC Mean ± Std Dev	0.331 ± 0.026	2.45 ± 0.18

Table 1: Package styles tested using TDIM and steady-state Theta jc methods

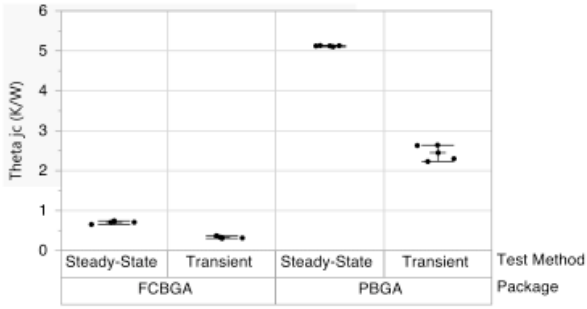

Figure 4: Comparison of Theta jc measurement methods for FCBGA and PBGA packages

Since the focus of this study is the application of comparative metrics, the actual Theta-JC value is less important than the precision in measuring changes in its value. Measurements should be repeatable regardless of the measurement method, but a consistent testing approach is required, for either a transient or steady-state Theta-JC method. For the FCBGA and PBGA packages tested, both the transient and steady-state methods yielded repeatable Theta-JC measurements.

What Causes TDIM Theta-JC To Be Lower Than Steady-State Theta-JC?

Finite Element Analysis (FEA) simulations are used to explain why the measured TDIM Theta-JC values are similar to steady-state Theta-JC values for one-dimensional conduction, and smaller when multi-dimensional conduction is present.

Thermal simulations were run for the TO247 package shown in *Figure 2* to predict the Z_{th} versus time. The model consists of a die bonded with solder to a die paddle that acts as a heat spreader. The package has three leads: the source, the drain and the gate. The package is overmolded with a low conductivity epoxy. A TIM is inserted between the exposed surface of the die paddle and the cold plate. A uniform heat flux is applied to the top surface of the die and a large convective heat transfer coefficient, e.g. 1000W/m^2, is applied to the base of the cold plate.

Temperature distributions are plotted in *Figure 5* for different distances measured from the top of the mold cap vertically along a line centered at the die. At approximately 7msec, the case temperature begins to increase above its initial zero power temperature. At this time, the wet and dry curves in *Figure 3* separated and the Z_{th} predicted by *Equation (5)* is equivalent to Theta-JC predicted by *Equation (1)* since $T_c = T_{j,t=o}$.

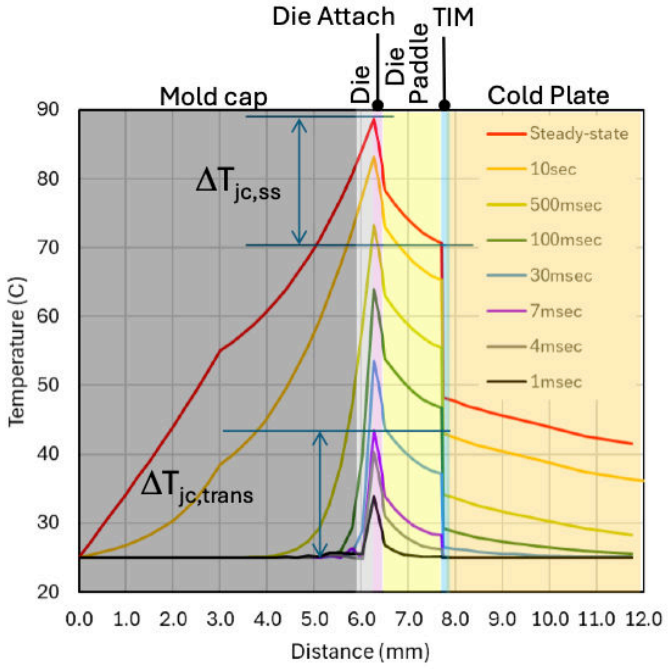

Figure 5: TO247 temperature variation along a line through center of die, P = 80W

At later times, the temperature difference between the case and junction remains constant, even after reaching steady-state conditions, see $\Delta T_{jc,trans}$ at early times is approximately equal to $\Delta T_{jc,ss}$ at later times. For the TO247 package, over 99% of heat flows into the cold plate with the rest flowing to the top of the package or the leads.

The transient analysis was repeated for the FCBGA package shown in *Figure 6*. Unlike the TO247, there are two resistance paths having similar orders of magnitude: one to the cold plate and a second to the JEDEC board.

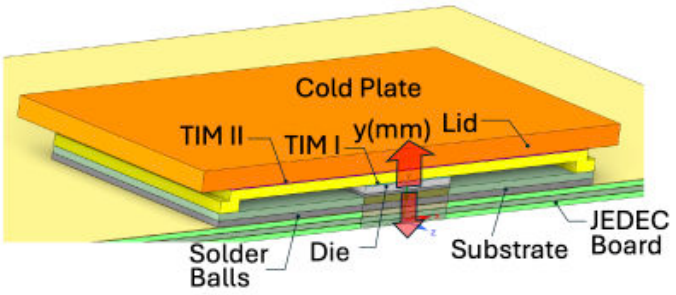

Figure 6: FCBGA FEA model

At the point of separation of the wet and dry Z_{th} curves, at approximately 0.1sec as shown in *Figure 7*, Z_{th} is approximately 0.30K/W.

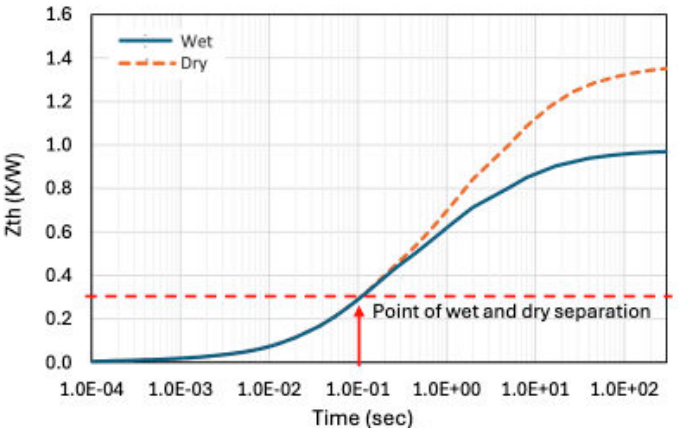

Figure 7: FCBGA simulated Z_{th} curve separation

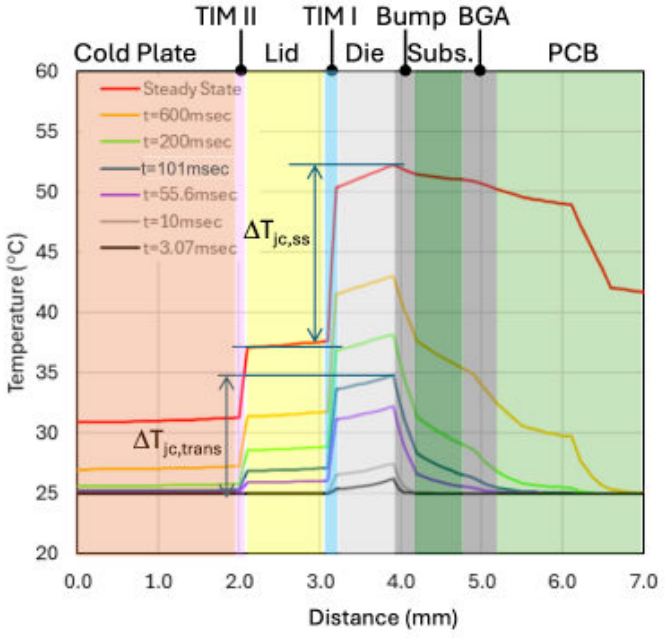

Figure 8: FCBGA temperature variation along a line through center of die, P = 60W

Temperature distributions along a vertical line centered at the die were predicted at several times ranging from 3.07msec to steady state, see *Figure 8*. At 101msec, the case temperature begins to increase at the same point in time when the dry and wet curves separate as shown in *Figure 7*. At steady state the temperature difference between the junction and case, $\Delta T_{jc,ss}$, is higher than the transient temperature difference, $\Delta T_{jc,trans}$. The junction-to-case temperature difference for steady-state is $\Delta T_{JC,ss}$ =15K compared to transient $\Delta T_{JC,trans}$= 9K, as shown *Figure 8*.

The large difference between TDIM and steady-state Theta-JC is attributed to multi-dimensional heat flow. The two-resistor model discussed in JESD51-3 [4] may be used to indicate if multi-dimensional heat flow is present. Theta-JC represents the restriction of heat flowing to the case and Theta-JB represents the restriction of heat flowing to the motherboard. When Theta-JB is much larger than Theta-JC, heat flow is primarily one-dimensional to the case. Bornoff [10] showed that, when Theta jb is at least 10X larger than Theta-JC, multi-dimensional heat flow effects are small and TDIM Theta-JC is similar to steady-state Theta-JC.

Theta jb predictions for the package shown in *Figure 6* are approximately 6 times the Theta-JC value. Due to multi-directional heat flow, a large difference between transient and steady-state Theta-JC can be expected.

Steady-State Theta-JC Testing Criteria

When running steady-state tests for certain packages the temperature difference between the junction and case is 30K or more while the temperature drop between the case and cold plate is less than 4K. Even though probing the case temperature introduces measurement errors, the Theta-JC error can be managed by establishing a minimum Theta-JC limit.

A minimum steady-state test condition is developed by requiring the TIM resistance be less than 10% of the measured Theta-JC so that by applying this constraint, the TIM temperature drop is no more than 10% of the junction to case temperature drop. Likewise, from *Equation (5)*, the ΔT_c term uncertainty attributed to the case temperature is limited to less than 10% of Theta-JC.

A conservative estimate for the TIM thermal resistance is made by assuming one-dimensional heat transfer through the TIM bond line thickness, L, and thermal conductivity, K_{TIM}, with an effective area equivalent to the die area, A_{die}. In practice, spreading within the package increases the effective heat flow area. An approximation for the thermal resistance in the TIM layer is written in *Equation (7)*.

$$\theta_{TIM} = \frac{L}{K_{TIM}\, A_{die}} < 0.10 * \theta_{JC} \qquad (7)$$

Solving *Equation (7)* for $\emptyset_{JC}$ gives a lower limit on the ratio of bond line thickness to TIM conductivity (L/K_{TIM}) for a given die size, as shown in *Equation (8)*.

$$\theta_{JC,min} * A_{die} > 10 * \frac{L}{K_{TIM}} \qquad (8)$$

The $\emptyset_{JC}{}^{*}\, A_{die}$ metric is used to estimate minimum Theta-JC values allowable as a function of die area. Regions to the right of a given L/K line in *Figure 9* meet the minimum Theta-JC, criteria given by *Equation (8)*.

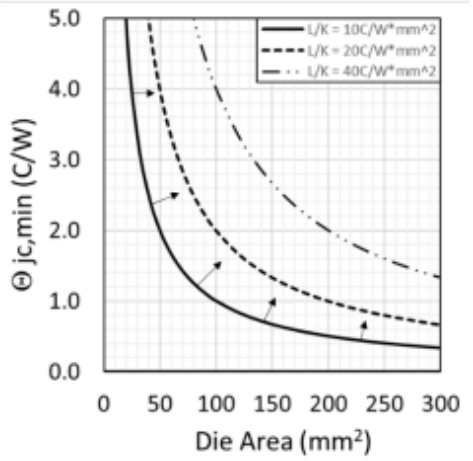

Figure 9: Valid $\emptyset_{JC}$ testing range as a function of die size

For high power and small area die, the large heat flux near the case temperature sensing location will cause a localized high temperature gradient in the TIM layer. Due to the uncertainty in case temperature measurements, there are restrictions in steady-state Theta-JC measurements for small area die. For example, the minimum die area allowable for $\emptyset_{JC}$ = 2.0°C/W in *Figure 9* is 100mm², provided L/K = 20°C/W*mm². Thermal greases have been reported to have L/K of 17-35°C/W mm² [11].

The thermal conductivity used in *Equation (8)* is an effective thermal conductivity and includes the contact resistances at the interfaces between the TIM layer and the case and the cold plate. Another challenge for measuring the case temperature is the presence of gradients in the TIM and across the case surface below the die. A good discussion of the challenges of measuring case temperature with a thermocouple is found in Pape, et.al. [12].

For certain package styles, case temperature measurement uncertainty can be reduced by embedding a temperature sensor into the case. For example, if the package has a case thickness greater than 1mm, then a fine gauge (0.5mm diameter) temperature sensor can be flush mounted to the outer surface of the case, see for example Galloway and de los Heros [13].

Conclusions

(i) Theta-JC may be used as a comparative metric for measuring relative thermal performance improvements between different suppliers or comparing thermal enhancements of different bill of materials.

(ii) Theta-JC can be used to quantify degradation in thermal performance as function of repeated stress conditioning.
(iii) Theta-JC measurements should be repeatable.
(iv) TDIM and steady-state Theta-JC tests may produce different values depending on the presence of multi-directional heat flow.
(v) When comparing thermal performance of two or more packages, the same testing method should be employed, i.e. do not mix steady-state and TDIM test results.
(vi) Steady-state Theta-JC test methods should be used with caution when Theta-JC is in the region to the left of curves shown in *Figure 9*.

References

[1] JESD51-12, "Guidelines for Reporting and Using Electronic Package Thermal Information", November 2012
[2] ECPE Guideline AQG 324 Qualification of Power Modules for Use in Power Electronics Converter Units in Motor Vehicles, March 2021, https://www.ecpe.org/index.php?eID=dumpFile&t=f&f=30359&token=cbab0d6a7844bb815684bcae699892313b924ddb
[3] Lasance, C., "Thermal resistance: an oxymoron?", Cooling Zone, December 2005. https://www.coolingzone.com/library.php?read=458
[4] Two-Resistor Compact Thermal Model Guideline, JESD51-3, July 2008
[5] DELPHI Compact Thermal Model Guideline, JESD51-4, July 2008
[6] Siemens Inc., "Embeddable BCI-ROM Technology: reduced order thermal models for 3D CFD electronics cooling simulation", https://blogs.sw.siemens.com/simcenter/embeddable-bci-rom-cfd-thermal-model/
[7] MIL-STD-883E, METHOD 1012.1, Thermal Characteristics, 4 November 1980
[8] JESD51-1, "Integrated Circuits Thermal Measurement Method – Electrical Test Method (Single Semiconductor Device", December 1995
[9] JESD51-14, "Transient Dual Interface Measurement – A new JEDEC Standard for the Measurement of the Junction-to-Case Thermal Resistance", https://www.jedec.org/standards-documents/docs/jesd51-14-0
[10] Bornoff R., "The applicability of JESD51-14 for the determination of junction to case thermal resistance", *Electronics Cooling Magazine*, March 2024, https://www.electronics-cooling.com/2024/04/the-applicability-of-jesd51-14-for-the-determination-of-junction-to-case-thermal-resistance/
[11] "Thermally conductive silicone grease compounds and pastes", https://www.momentive.com /en-us/industries/electronics/thermal/thermally-conductive-grease-compounds-paste
[12] Pape H., Schweitzer D., Chen L., Kutscherauer R. and Walder M, "Development of a Standard for Transient Measurement of Junction-To-Case Thermal Resistance", 12th Intl. Conf. on Thermal, Mechanical & Multi-Physics Simulation and Experiments in Microelectronics and Microsystems, 2011
[13] Galloway J. and de los Heros E. "Developing a Thetajc Standard Under Steady-State Testing Conditions", https://www.electronics-cooling.com/2018/03/developing-thetajc-standard-steady-state-testing-conditions/, March 2018


Call for Authors
and Contributors!
Want to be a part of the next issue of Electronics Cooling? Have an article or blog post you'd like to write for Electronics-Cooling.com?
Let us know at
editor@electronics-cooling.com
electronics COOLING
www.Electronics-Cooling.com

Index of ADVERTISERS

Electronics Cooling
716 Dekalb Pike, #351
Blue Bell, PA 19422

t: (484) 688-0300
e: info@electronics-cooling.com
w: electronics-cooling.com
page: 30

Lectrix
716 Dekalb Pike, #351
Blue Bell, PA 19422

t: (484) 688-0300
e: info@lectrixgroup.com
w: lectrixgroup.com
page: 32


Break the same old pattern.
Problem First. Product Last.
Content | Data | Marketing Technology
LECTRIX®
Digital Marketing for the B2B Electronics Industry
1.484.688.0300 | info@lectrixgroup.com
www.lectrixgroup.com